RF Project 765863/719176
Technical Report

A REVIEW OF GEAR HOUSING DYNAMICS AND ACOUSTICS LITERATURE

Rajendra Singh
Department of Mechanical Engineering

Teik Chin Lim
Graduate Research Associate

For the Period
March 1987 - December 1987

NATIONAL AERONAUTICS AND SPACE ADMINISTRATION
Lewis Research Center
Cleveland, Ohio 44135

Grant No. NAG3-773

July 1988

The Ohio State University Research Foundation
1314 Kinnear Road
Columbus, Ohio 43212

A REVIEW OF GEAR HOUSING DYNAMICS AND ACOUSTICS LITERATURE

Teik Chin Lim
Graduate Research Associate
Department of Mechanical Engineering

Rajendra Singh
Professor
Department of Mechanical Engineering

For the Period
March 1987 – December 1987

NATIONAL AERONAUTICS AND SPACE ADMINISTRATION
Lewis Research Center
21000 Brookpark Road
Cleveland, Ohio 44135

Grant No. NAG3-773

July 1988

Table of Contents

Summary

A review of the available literature on the gear housing vibration and noise radiation is presented. Analytical and experimental methodologies used for bearing dynamics, housing vibration and noise, mounts and suspensions, and the overall geared and housing system are discussed. Typical design guidelines as outlined by various investigators will be given.

A. Introduction [1-7]

The gearbox vibration and noise are caused by the dynamics of gear tooth meshing which can be characterized by the transmission error [1-4]. The transmission error is the deviation of gear angular position from its ideal location due to tooth profile and spacing error, and elastic deformation of gear teeth and body. Its magnitude is of the order of several microns. This action produces gear tooth dynamic forces at mesh frequency, f_{gm} (Hz) where

$$f_{gm} = N_g f_s \tag{1}$$

Here N_g is the number of gear teeth on the shaft rotating at speed f_s (Hz). Several harmonics of f_{gm} are also noted in measured data. Additionally one can get side bands at $f_{gm} \pm nf_s$ where n is an integer; here f_s can represent any shaft frequencies [4-6].

These forces excite coupled torsional/axial/transverse vibratory modes of the gear shafts and produce lateral and vertical displacements at the support bearing locations. Dynamic bearing forces are then generated due to the relative motions across the bearings in the radial direction. These in turn cause housing vibration and noise radiation at all mesh frequencies. In most cases, the noise radiation from the gear housing is due to flexural or bending vibrations of the housing walls [7]. The characteristic of such a wave motion is shown in Figure 1. If the transmissibilities of the mounts and suspensions are high, they may serve as paths for the structure-borne noise and vibration from the housing to structures attached. These structures will vibrate and/or radiate noise too. This vibration and noise generation mechanism for a typical planetary geared system is shown in Figure 2 [4,8]. The pulsating force form over a one tooth spacing cycle generated at the gear teeth in contact for each pair of meshing gears is also shown in this figure.

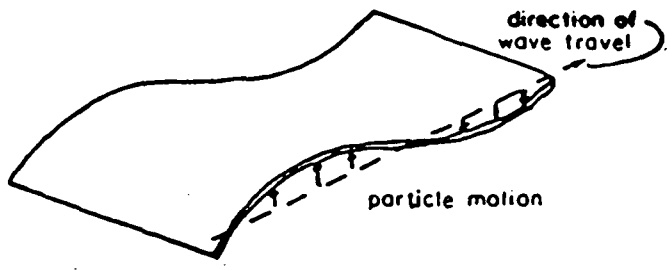

Figure 1. The flexural or bending wave is also a transverse wave, but in this case the motion is perpendicular to both the direction of wave travel and the free surfaces [7]

There have been numerous efforts since the 1960's to model gearbox dynamics and acoustics analytically, empirically, and experimentally. Analytical and experimental methodologies have been applied extensively to model the dynamics of geared transmission system. Some of these models have included the dynamics of gear housing. However, most of the gearbox noise prediction models have been semi-empirical in nature due to the complexity of the noise generation mechanism; and there have been many experimental programs undertaken to characterize the noise field. The purpose of these studies [7-19] have been to predict and control gearbox vibration and noise radiation. Ultimately, the goal is to obtain an optimal gearbox design which minimizes its vibration and noise radiation.

This review presents previous experimental and analytical methodologies used for shaft-bearing dynamics, housing dynamics and acoustics, gearbox mounts and suspensions, and the overall geared and housing system. These will include a discussion of various formulations and assumptions. Typical results and problem areas regarding the techniques used will be pointed out. Some of the typical design criteria reported by various investigators are also summarized.

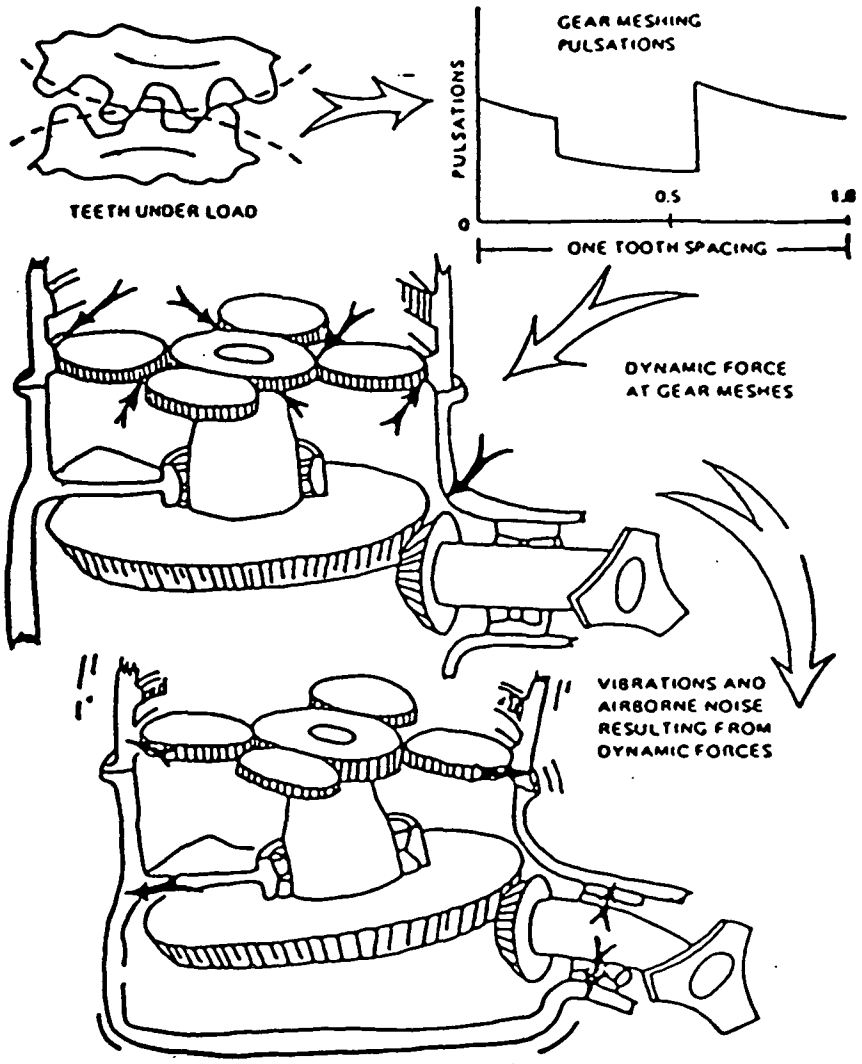

Figure 2. Gearbox vibration and noise generation mechanism [4,8]

B. Gear-Shaft-Bearing Dynamics [7-37]

Gears and shafts vibrations produce bearing reaction forces. These forces are responsible for transferring the displacement form of excitations of meshing gears to the housing. Knowing the nature of these forces and their transfer paths will allow better control and prediction of the gearbox vibration and noise. A detailed review of the gear dynamics models has been conducted by Ozguven and Houser [20].

Laskin, Orcutt and Shipley [9,10], in 1968, used the Holzer torsional vibration models of simple and planetary gearing system to compute gear tooth dynamic forces. A segment of this torsional vibration system is shown in Figure 3. Based on this model, two

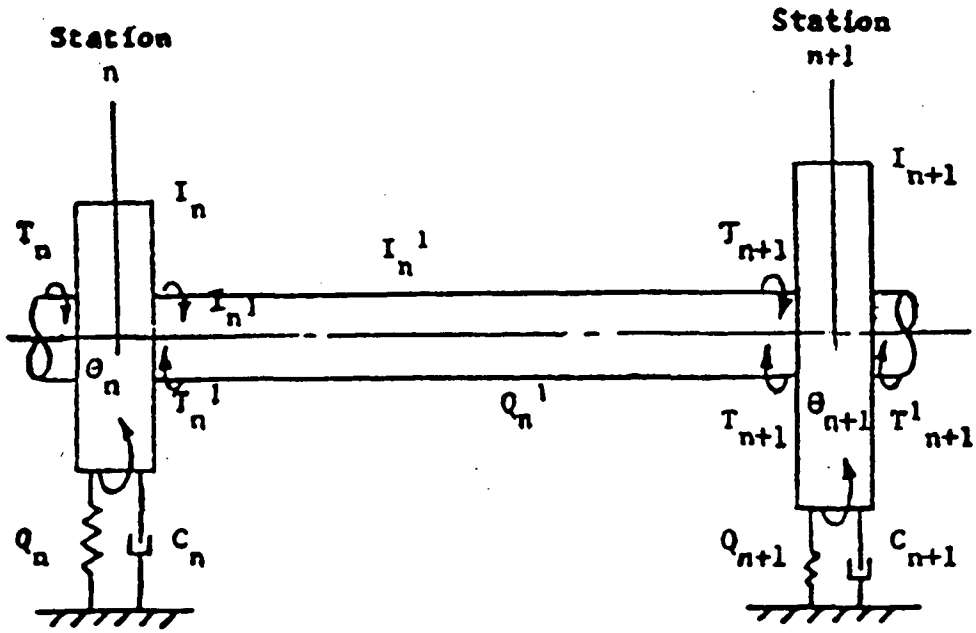

I = mass moment of inertia Q = torsional compliance

T = torque C = damping

θ = angular motion

Figure 3. General portion of the Holzer torsional system. Subscript n and n+1 indicate station number.[9]

relationships for the angular motion and torque between successive stations and at each station were obtained. One equation described the transfer of angular motion and torque between stations while the other described the difference between the input torque and the output torque at each station. They applied this method, in conjunction with a gear excitation model and experimental data, to study the vibration energy paths of the UH-1D helicopter transmission. Badgley and Laskin [11,12], in 1970, performed similar experimental and analytical studies on the CH-47 helicopter transmission.

Badgley and Chiang [13-15], in 1972, used a shaft-bearing system dynamics approach to obtain the lateral response of a gear support system. Using this approach bearing dynamic forces may be obtained from the previously computed gear tooth dynamic forces [9-12]. This analysis was performed upon the assumption that transverse vibration of the shafts are responsible for transferring the gear tooth dynamic loads to the housing. Moreover, the lateral resonance frequencies are within the gear mesh frequency range, that is, in the order of a kiloHertz. Finite cylindrical beam elements with rotation and lateral degrees of freedom were used to model the system. Nonisotropic linear bearings, and uncoupled torsional and lateral motions of the system were assumed. Effects of housing flexibility on the gear-shaft dynamics were not included.

Experimental evaluation was done in parallel with these analytical predictions. Qualitative results for gear mesh frequencies, vibration levels, etc. were in good agreement with the experimental data. However these methods do not indicate the effectiveness of a gearbox design change in terms of vibration and noise reduction in the audible frequency range as shown by Sternfeld, Schairer and Spencer [16].

Bowes et. al. [17-19], in 1977, reviewed and modified previously constructed analytical models by Badgley and Chiang to include the dynamical effects of housing mass, stiffness, and damping. Holzer-Myklested technique was used to model the uncoupled torsional and flexural vibrations of the geared system with shafts as slender cylindrical

beams and the gears as lumped masses and inertias. A typical model is shown in Figure 4 where each shaft segment was treated as uniform torsion-flexure element with distributed inertia. The model has N shaft segments with N+1 stations.At each station, a rigid body of

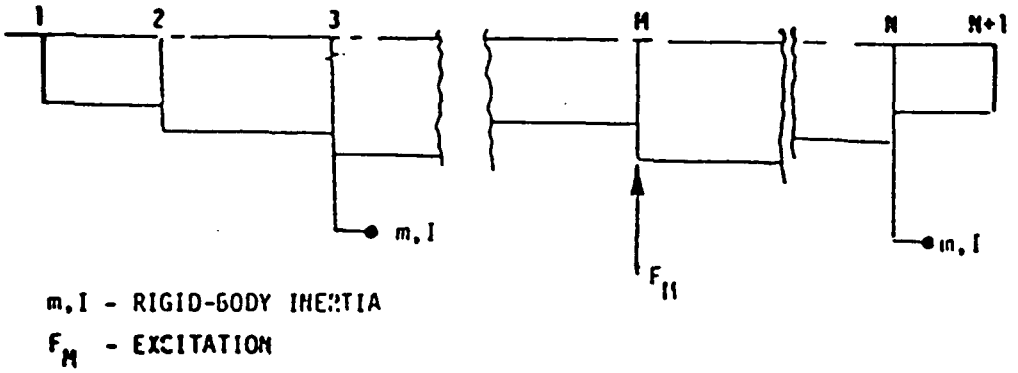

Figure 4. Geared system representation [19]

mass m and mass moment of inertia I, and/or an excitation F_M may be attached. Due to the assumption that the torsional motion is uncoupled from the lateral motion, both the related impedance matrices were obtained separately. Using the transfer matrix approach, the mechanical impedance of the total geared system was constructed such that [19]

$$\begin{Bmatrix} F_1 \\ F_2 \\ F_3 \end{Bmatrix} = \begin{bmatrix} [z_{11}] & [z_{12}] & [0] \\ [z_{21}] & [z_{22}] & [0] \\ [0]^T & [0]^T & [z_{33}] \end{bmatrix} \cdot \begin{Bmatrix} x_1 \\ x_2 \\ x_3 \end{Bmatrix} \tag{2}$$

where $[z_{ij}]$ = impedance submatrix relating responses in the i direction to excitations in the j direction

$[0]$ = null submatrix

x_i = responses in the i direction

F_j = excitations in the j direction

i , j = 1, 2, 3

with 1 = vertical direction

2 = horizontal direction

3 = angular torsional direction

This resultant impedance matrix was then combined with the housing impedance, which will be discussed later, using the component synthesis method. The bearings models were nonlinear springs in the two orthogonal directions considering bearing geometry, torque, and shaft speed [17-19,21]. The SH-2D helicopter transmission were analyzed [17-19].

Salzer, Smith and Welbourn [22,23], in 1975 and 1977, simulated a 6 degrees of freedom lumped-mass model of an automobile gearbox internal components independent of the housing parameter on an analog computer. The system and its simulation block diagram are shown in Figure 5 and 6 respectively. An analog model was used. The computed

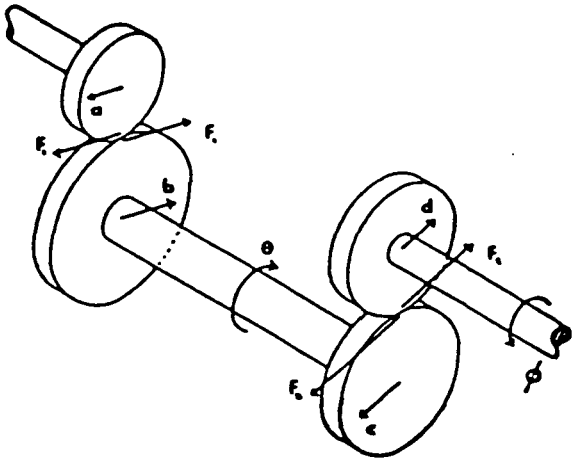

Figure 5. Idealization of the automobile gearbox internal components [22]

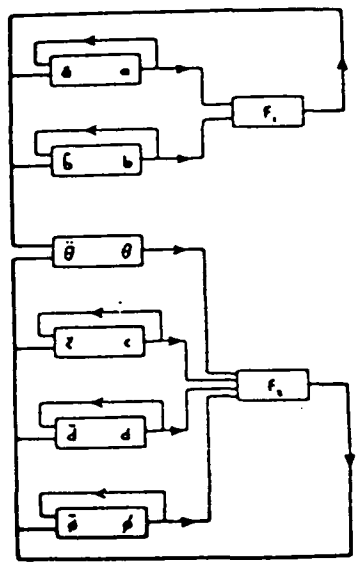

Figure 6. Block diagram of gearbox vibration simulation [22]

bearing forces were available immediately for audible output through a loudspeaker. The results were found to be very similar in character to the experimental data when seen in the frequency domain but the magnitudes were not the same. Astridge and Salzer [24], in 1977, also used partial lumped-mass method to model the vibrations of the Wessex Tail Rotor gearbox as illustrated in Figure 7. Thirteen lumped mass locations numbered 1 thru 13 were selected and each has 6 degrees of freedom. All the shafts and part of the housing were modeled as hollow cylindrical beams. However, the stiffness matrix of the complex housing section was obtained using the finite element method. Sinusoidal forced response analysis indicated very little relative displacement across the bearings since the shafts and housing virtually moved together, and the dynamic bearing loads were about 5% of the static loads.

Recently, Neriya, Bhat and Sankar [25] used the lumped-mass model to include the coupled torsional and lateral vibrations of a simple gear-shaft system as illustrated in Figure 8. At the bearing locations, the simply supported boundary conditions were assumed.

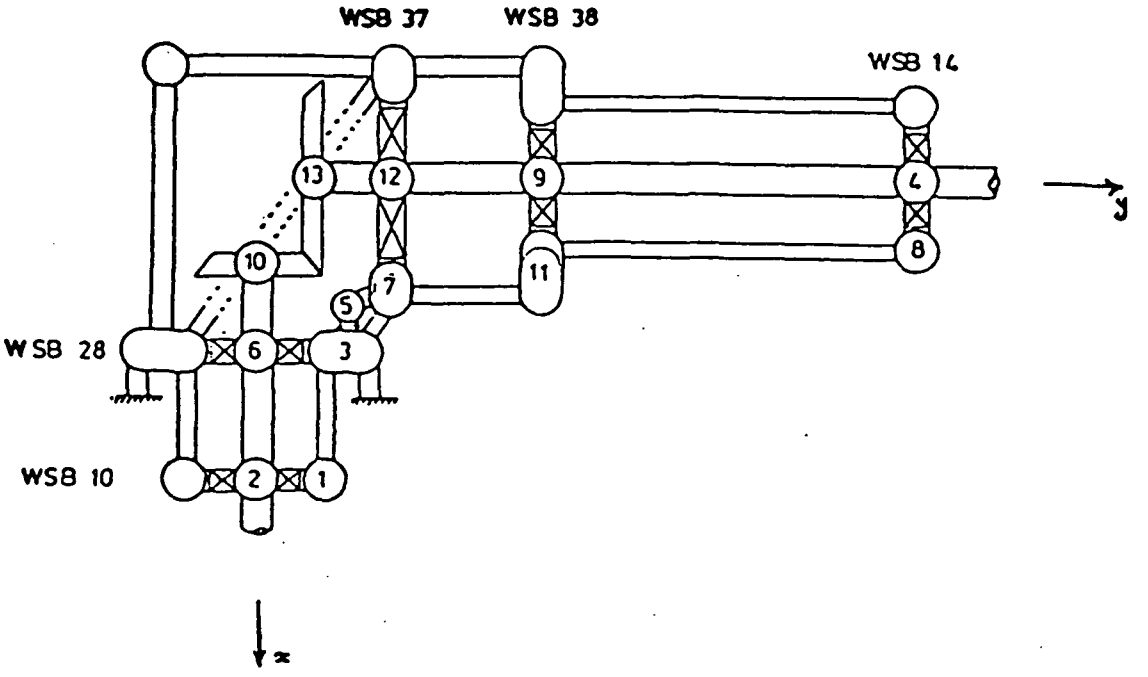

Figure 7. Wessex Tail Rotor Gearbox model idealization and the location of lumped-masses and inertias [24]

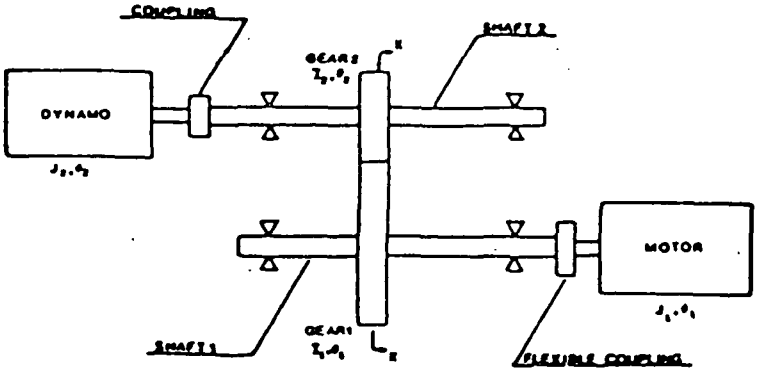

Figure 8. Simple gear-shaft system [25]

A lumped parameter model of dynamometer, motor, shaft stiffnesses, and gears was used to obtain a set of second order dynamic equations [9]

$$[M]\{\ddot{q}\} + [C]\{\dot{q}\} + [K]\{q\} = \{F\} \tag{3}$$

where $[M]$ = generalized mass matrix

$[C]$ = generalized damping matrix

$[K]$ = generalized stiffness matrix

$\{q\}$ = generalized displacement vector

$\{F\}$ = generalized force vector

Using the normal mode analysis method, the dynamic tooth loads were estimated to be maximum at the torsional resonances which concluded that coupling between the torsional and lateral vibrations did not have significant effect on this behavior.

The finite element method (FEM) was also used to model the internal components of geared transmissions. These models were usually assumed to be uncoupled from the housing like most of the above ones by the assumption that the gear-shaft system is much more flexible than the housing. Hartman [26] used the finite element method to model the transverse-torsional-axial vibration of the 301 HLH/ATC helicopter geared transmission. The dynamic tooth forces computed using the approach adopted by Laskin, Orcutt, and Shipley [9] were used as inputs in the forced response analysis. He indicated that the finite element approach has the advantage of allowing coupling between adjacent shafts across the gear meshes by defining gear mesh stiffnesses.The gears were modeled as lumped masses and inertias with linear springs between the nodes, shafts were modeled as beams, and bearings were modeled as beams and springs. Sciarra et. al. [8,27], Drago [28], and

Royal, Drago and Lenski [29] used similar finite element program to model the CH-47 helicopter geared transmission as illustrated in Figure 9.

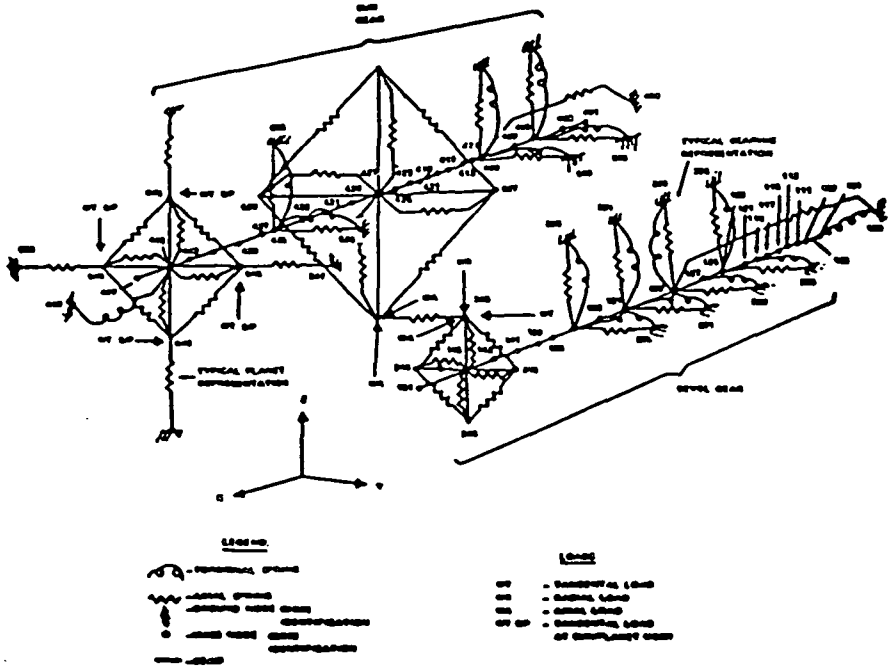

Figure 9. Finite element model of the CH-47 geared transmission [28]

In addition, the strain energy densities at each mesh frequency were computed to identify possible design alterations. Observations of the first 20 mode shapes indicated that most of them are primarily coupled bending/torsion modes. The bearing forces computed were used to excite the NASTRAN finite element housing model. These loads were phased at each mesh frequency due to damping.

Neriya, Bhat and Sankar [30] specifically studied the effect of coupled torsional-transverse vibration of a simple gear shaft system, also shown in Figure 8, now using 41 degrees of freedom finite element model. A typical beam element with 6 degrees of freedom is shown in Figure 10. Nonisotropic bearings elements were assumed by specifying linear stiffnesses in two orthogonal directions in the plane of the support bearings. Typical stiffness is approximately 10^8 N/m. However, the basis for obtaining the equivalent damping coefficient in each mode is not clear.

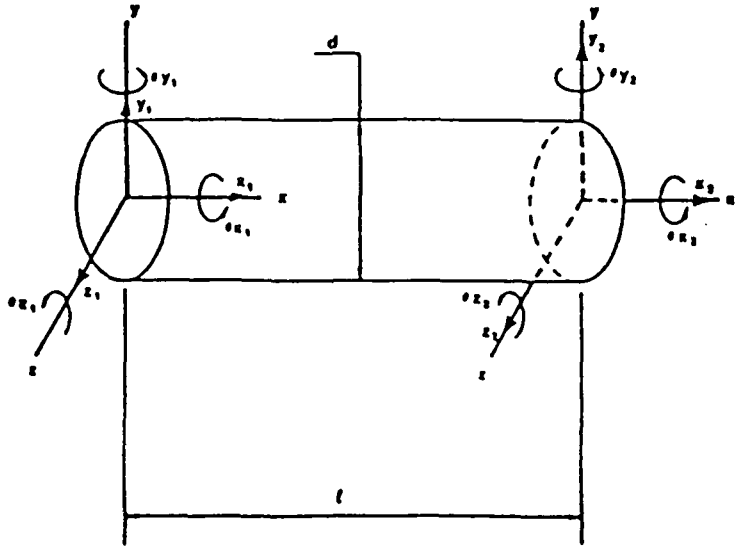

Figure 10. Typical beam element used in rotor dynamics [30]

Steyer [31], 1987, mentioned that a detail analysis of a geared transmission would take up a lot of time and also require some modeling experience. He then suggested an impedance analysis of a simple gear-shaft system independent of housing parameters for dynamic bearing forces estimation. This was done by assuming a large impedance mismatch at the support bearings. First, the excitation at the mating teeth, F_{mesh}, was given by the product of the mesh impedance, Z_{mesh}, and the relative velocity between mating teeth, $i\omega\delta$. The mesh impedance was evaluated in terms of the impedances of the shafts for the translational and rotational components, and the lateral vibration of the shaft at the bearing location was given as [31]

$$x_1 = F_{mesh}\, Z_{T1}^{-1} / i\omega \qquad (4)$$

where Z_{T1}^{-1} = mobility of shaft 1 (translational)

ω = angular velocity

$$i = \sqrt{-1}$$

Defining a bearing stiffness, $K_b(\omega)$, the bearing force [31]

$$F_b = x_1 K_b \tag{5}$$

The final form of the bearing force for identical shaft 1 and 2 was shown to be [31]

$$F_b = K_b \delta [Z_T (i\omega K_M^{-1} + 2Z_R^{-1}) + 2]^{-1} \tag{6}$$

where Z_T = shaft translational impedance

Z_R = shaft rotational impedance

Z_M = tooth compliance

The bearing response based on this model is shown in Figure 11. The response was

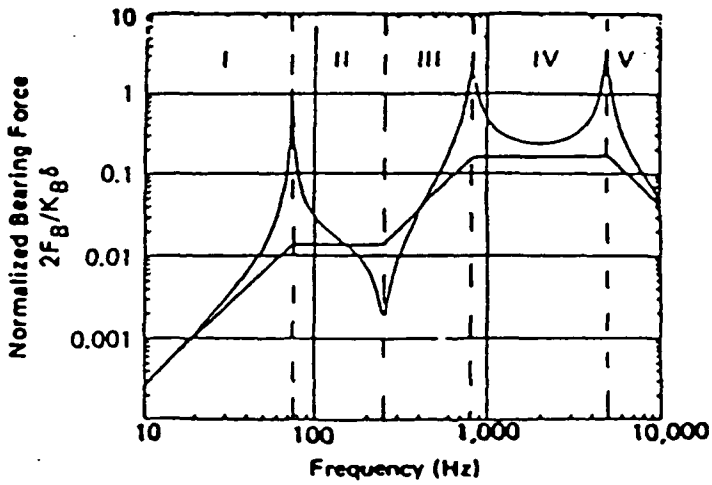

Figure 11. Typical force transmissibility curve (exact and asymptotic) [31]

divided into 5 regions which are also tabulated in Table 1. Each region has its own controlling factor, for example, the response in region IV is proportional to the ratio of the gear torsional inertia to the sum of inertia and mass, and the response in region III is proportional to the gear torsional inertia.

Table 1. Frequency limits and approximate response for the 5 regions [31]

Zone	$2F_B/K_B\delta$ / $\omega^2 (J_G + J_R)/R^2 K_T$	Frequency Limits
I		$\omega^2 = 0$
II	$K_R/(K_T + K_R)$	$\omega^2 = K_R/(J_G + J_R)$
III	$\omega^2 J_G/R^2 K_T$	$\omega^2 = K_R (J_G^{-1} + J_R^{-1})$
IV	$J_G/(R^2 M + J_G)$	$\omega^2 = K_T/M$
V	$K_T/(M\omega^2)$	$\omega^2 = 2K_M(M^{-1} + R^2 J_G^{-1})$
		$\omega^2 = \infty$

where
- M = Shaft effective mass
- K_T = Shaft lateral stiffness
- R = Gear pitch radius
- J_G = Gear torsional inertia
- K_R = Shaft torsional stiffness
- J_R = Reaction torsional inertia

In the previous mathematical models for the vibration energy transfer through the bearings, only radial forces were assumed acting through the bearings. Rajab [32] allowed radial and moment loads transmitted through the support bearings. The sketch of the ball bearing model used is shown in Figure 12. Bearing angular and radial stiffnesses were obtained by solving a set of approximate bearing-shaft load-deflection equations using the

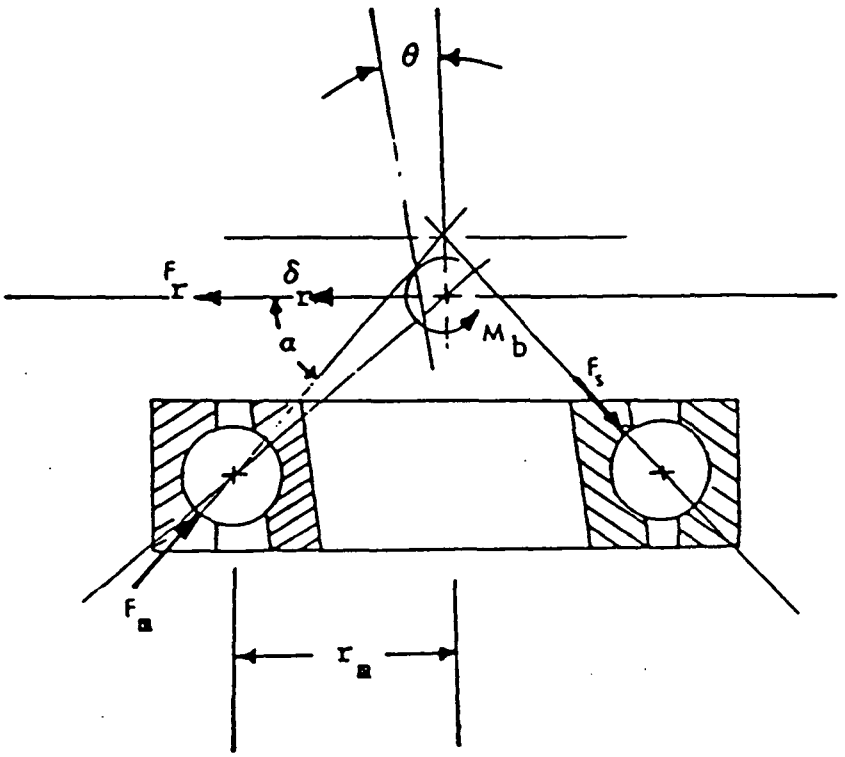

F_m = maximum load θ = angular deflection

F_r = radial load δ_r = radial deflection

M_b = moment load r_m = pitch radius

Figure 12. A bearing under radial and moment load [32]

Newton-Raphson iteration method. The solution for the bearing radial force F_r, and moment M_b were used to define the bearing stiffness elements as [32]

$$K_{rr} = \frac{F_r}{\delta_r} \quad \text{lbf./in.} \tag{7}$$

$$K_{r\theta} = \frac{F_r}{\theta} \quad \text{lbf./rad.} \tag{8}$$

$$K_{\theta r} = \frac{M_b}{\delta_r} \quad \text{lbf. in./in.} \tag{9}$$

$$K_{\theta\theta} = \frac{M_b}{\theta} \quad \text{lbf. in./rad.} \tag{10}$$

These results compared well with the manufacturer data. A typical comparison is shown in Figure 13 for the radial deflections for some radial loads. In addition, a review of the mathematical models of the bearings is also presented by Rajab [32].

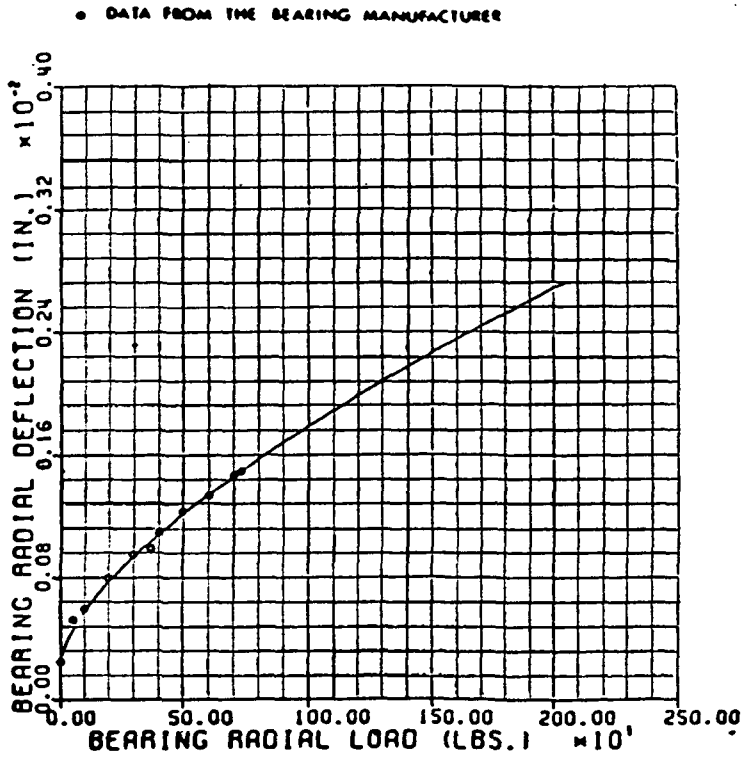

Figure 13. Bearing radial deflection for some radial load [32]

This model was then used in the building-block system analysis of the shaft-bearing-plate model to study the force/motion transmissibility through the support bearings. Related experimental studies were performed on a single shaft supported by a flat rectangular plate

through a radial contact bearing. The plate was clamped at all the edges as illustrated in Figure 14.

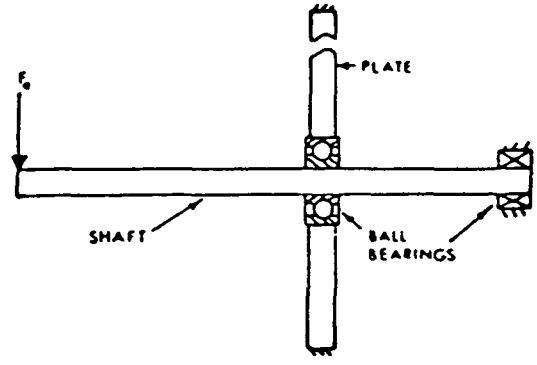

Figure 14. Shaft-bearing-plate setup for bearing transmissibility studies [32]

Taha [33] also analyzed bearing transmissibility using a set of load-deflection equations of the shaft-bearing-housing system. The deflection of the housing was taken into account when computing the radial and moment loads across the bearings. These analysis were only used to study the effect of bearing misalignment on the performances of the gearbox such as shaft deflection and bearing life. The Wessex Tail Rotor gearbox was analyzed as an example.

The statistical energy analysis (SEA) method has been used to analyze power flow in marine geared transmission from the gears to the housing [7,34]. This SEA approach is valid when the modal density is high. A complex system like a gearbox can be divided into many subsystems. An energy balance is then performed on the entire system by considering energy stored, energy loss to the environment and energy transfer from one subsystem to another. The response of each subsystem is computed in terms of the average

and standard deviation of the rms response in a frequency band. Lu, Rockwood and Warner [34] developed an SEA model of a marine gear-turbine system, using 79 subsystems and 148 junctions schematically shown in Figure 15, for comparison with the finite element method (FEM). The result is shown in Figure 16.

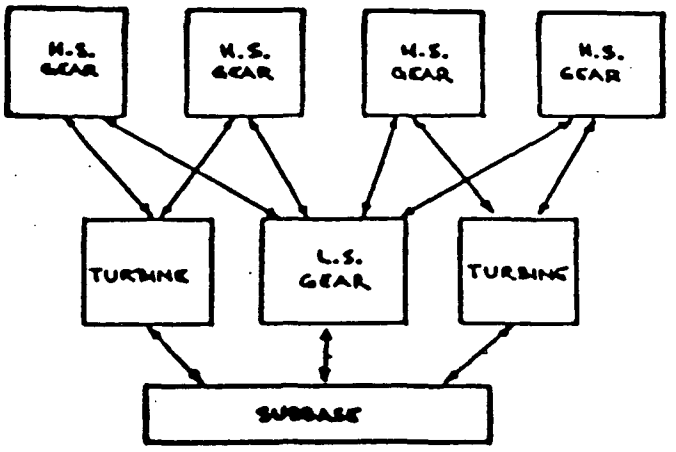

Figure 15. SEA model of a marine gear-turbine system [34]

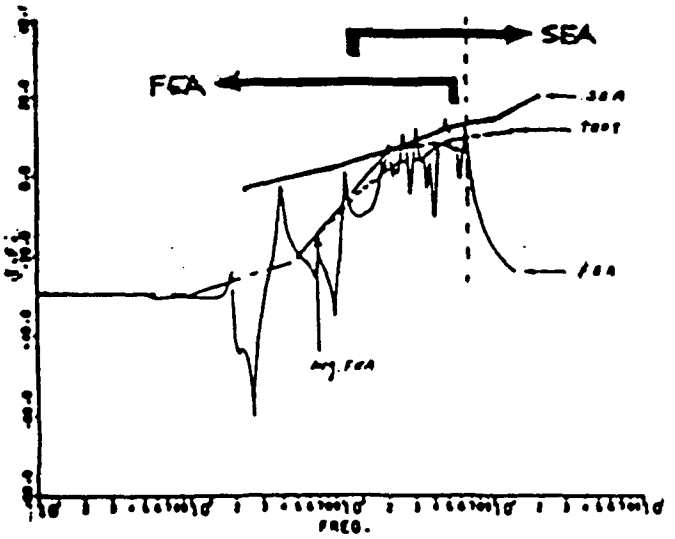

Figure 16. Analytical method applicable range [34]

The SEA method is obviously preferred in the high frequency range because it is not affected by the increase in the number of participating modes as in the FEM. The general power flow equation based on the SEA method is given as [34]

$$\begin{bmatrix} \eta_1 + \sum_{2}^{N}\eta_{1j} & -\eta_{21} & \cdots & -\eta_{N1} \\ -\eta_{12} & \eta_2 + \sum_{1,3}^{N}\eta_{2j} & \cdots & -\eta_{N2} \\ \cdot & \cdot & \cdots & \cdot \\ \cdot & \cdot & \cdots & \cdot \\ \cdot & \cdot & \cdots & \cdot \\ -\eta_{1N} & \cdot & \cdots & \eta_N + \sum_{1}^{N-1}\eta_{Nj} \end{bmatrix} \begin{Bmatrix} E_1 \\ E_2 \\ \cdot \\ \cdot \\ \cdot \\ E_N \end{Bmatrix} = \begin{Bmatrix} \pi_{in}^1 / \omega \\ \pi_{in}^2 / \omega \\ \cdot \\ \cdot \\ \cdot \\ \pi_{in}^N / \omega \end{Bmatrix} \tag{11}$$

where η_i = The loss factor of subsystem i

η_{ij} = Coupling loss factor

E_i = Energy stored in the subsystem

π_{in}^i = Input power

ω = Frequency (rad / sec)

Lyon [7] also used the SEA method to estimate the transfer functions for the energy transfer paths in a marine gearbox. He showed that the SEA prediction was better than than the lumped-mass model when compared with a 1/4 scale model.These comparison are shown in Figure 17.

In other experimental studies, Ishida, Matsuda and Fukui [35] studied the transmission of vibration energy in an automobile gearbox by examining the acceleration and noise frequency spectra at various location of the gearbox and its surrounding. A schematic of the vibration and noise transmitting paths is shown in Figure 18. It was also found that most (95%) of the total gearbox noise came via the structure-borne paths where

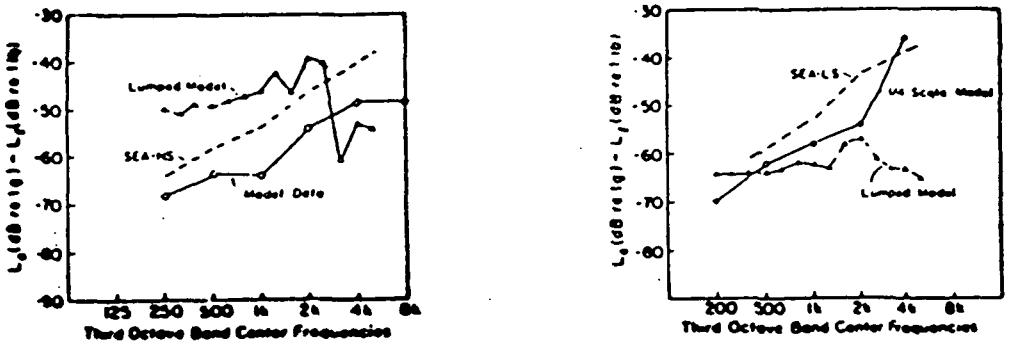

Input mesh to housing

Output mesh to housing

Figure 17. Analytically and experimentally obtained transfer function (gear to housing) of a marine gearbox [7]

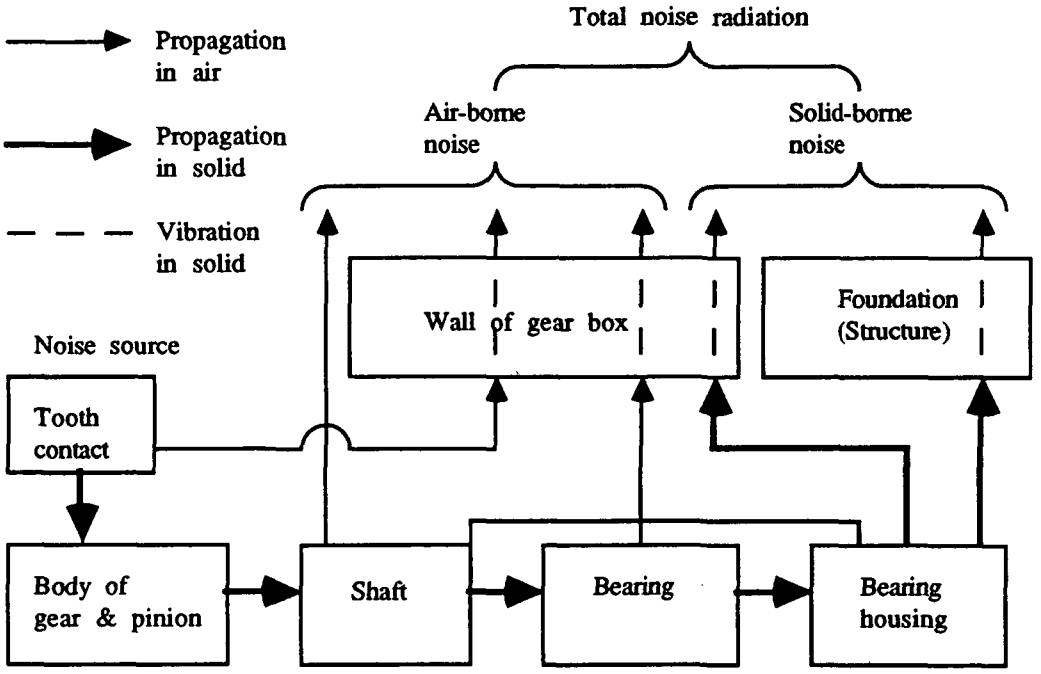

Figure 18. Vibration and noise transmitting paths in an automobile gearbox [35]

the fraction $E_D \approx 95$ % was computed as

$$E_D = E_S / (E_S + E_A) \tag{12}$$

where E_A = output energy density through air-borne path

E_S = output energy density through solid-borne path

The output energy densities were computed from the mean noise reductions for the air-borne, solid-borne, and total noise. This high structure-borne noise contribution is due to the fact that most of the air-borne noise from the meshing gears was reduced by the housing. In addition, a free torsional vibration analysis using Holzer's method was also performed on this multispeed geared transmission.

Randall [36,37] suggested examining the vibration data in the cepstrum domain to extract certain information on the gearbox vibration which otherwise cannot be obtained from the frequency (spectrum) and time domains. The cepstrum is an inverse Fourier Transform of the logarithmic power spectrum, or mathematically [36]

$$C(\tau) = [\Im^{-1}\{\log F(f)\}]^2 \tag{13}$$

where $C(\tau)$ = cepstrum

$F(f)$ = power spectrum of the time signal

$\Im^{-1}\{\ \}$ = inverse Fourier Transform

This cepstrum analysis was reported to allow one to extract periodicity in the spectrum, detect increase in sidebands amplitude and spacing which usually implies deterioration of geared transmission, analyze spectra of very fine resolution, separate excitation from the

vibration transfer path function, etc. Randall [37] used cepstrum analysis to obtain the excitation and its transfer path functions from the measured response of a gearbox. This could be done because the cepstrum of the measured response being a sum of the excitation and its transmission path cepstra. Also the excitation was found to concentrate at higher quefrency range as compared to the transmission path function. To show this application, consider the spectrum of the measured response [37]

$$F(f) = G(f) * H(f) \tag{14}$$

where G(f) and H(f)are the excitation and impulse response spectra. Hence, the Fourier Transform of logarithmic measured response function in equation (14) is [37]

$$\Im^{-1}\{\log F(f)\} = \Im^{-1}\{\log G(f)\} + \Im^{-1}\{\log H(f)\} \tag{15}$$

i.e. the sum of source and impulse response cepstra is the measured response cepstrum. A typical cepstrum is shown in Figure 19. The excitation can be seen to dominate at the high

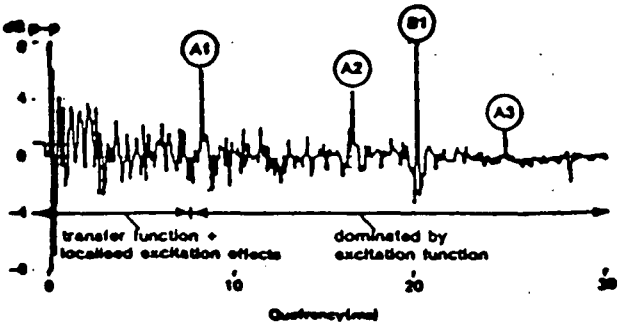

Figure 19. Measured response cepstrum [37]

quefrency range. Once the region of low quefrency range where the effects of the impulse response is significant is determined, it is possible to curve fit the response to a transfer function with known number of poles and zeroes. This can then be subtracted from the total cepstrum leaving only the excitation cepstrum. These cepstra can then be transform back to the frequency or time domains for diagnostic.

Lyon [7] performed mode counts on a gear and shaft to study the vibration transfer in these structures. He showed that at high frequency, part of the gear-shaft system acts as a 2 dimensional structure resulting in a higher number of participating modes. For example, Figure 20 indicates that the hub of the gear display new circumferential modes, in addition to the 1 dimensional shear and bending modes, at frequency above 16 kHz. On the other hand, the bending, and inplane longitudinal and shear vibrations of the rim of the gear occurs at all frequencies.This occurrence of additional modes result in higher ability in the structure to transfer vibration energy.

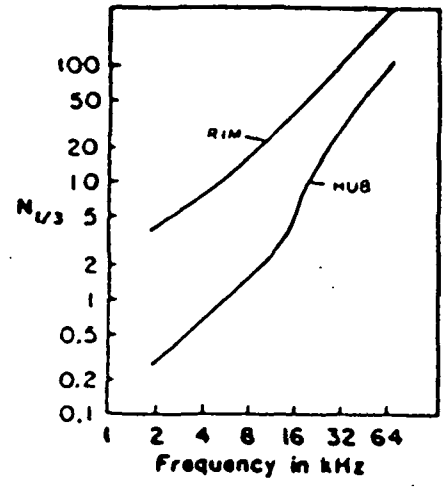

Figure 20. Mode counts in third-octave bands for rim and hub of a gear [7]

C. Housing Dynamics [4,8-11,13,15-19,21,24,26,28,29,33,34,38-48]

A number of publications [8,9,11,13,16,18,21,26,35,38-45] contain experimental data on gear housing vibration due to gear excitation at the mesh frequencies and their multiples. Most of these give the transverse acceleration frequency spectra of the housing plates. Ishida, Matsuda and Fukui [35], and Lewicki and Coy [44] indicated that higher gearbox operating speed implies higher average rms vibration of the housing walls. Also, others have realized that the measurement locations significantly affect the measured vibration due to change in vibration transfer path function from one point to another. On the other hand, housing vibration was found to be quite insensitive to change in geared transmission nominal input/output torque.

Although extensive experimental studies were undertaken, attempts to correlate these test results with analytical predictions were limited. One reason may be the complexity of the housing geometry involved, for example the CH-47 and UH-1D helicopter transmission described in the previous section. To date, modeling of gear housing vibration may be grouped as lumped-mass approach, analytical modal analysis, finite element method (FEM), and statistical energy analysis (SEA), etc. Some of these methods were combined to form a hybrid model and some were aided by other secondary methods in order to achieve a simple but reliable dynamic model.

One of the early effort to model a gear housing as a nonrigid structure where it was not coupled to the gear-shaft system was done in 1972 by Badgley and Chiang [13,15] in their continuous effort to predict and control helicopter gearbox vibration and noise. They applied thin shell theory to characterize the dynamics of finite cylindrical elements of variable thickness used in modeling the ring gear housing of the CH-47 and UH-1D helicopter transmission. The choice of this element was a natural one for the shape of the

gear housings with the ring gear. The CH-47 housing model composed of 3 cylindrical shell elements is illustrated in Figure 21. Simply supported conditions were assumed at the

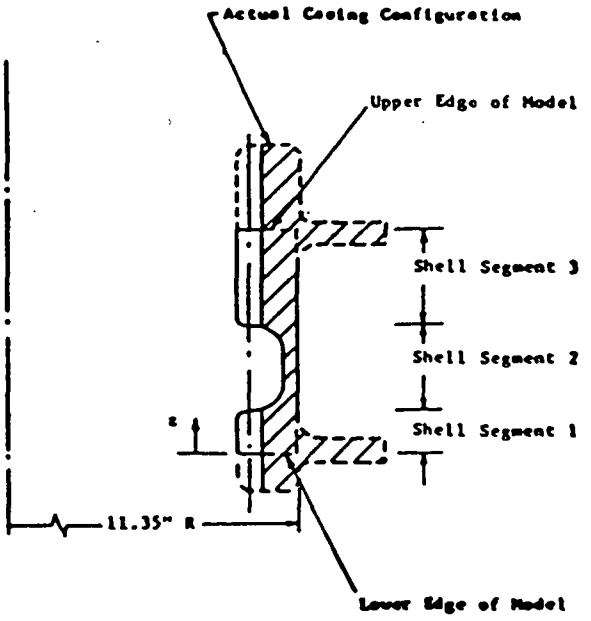

Figure 21. Ring gear housing model for the CH-47 helicopter transmission [13,15]

two edges which allowed only rotation about the circumference. Free and forced vibration were performed. In the free vibration analysis, axial and/or circumferential modes were found to dominate the behavior as expected. It was noted that although the housing is axisymmetric, some modes are not axisymmetric, like the 2nd circumferential mode shape in which the amplitude repeats itself twice per revolution shown in Figure 22. An example of the first and second axial modes are illustrated in Figure 23. Typical natural frequencies of the housing are tabulated in Table 2. Comparison of these natural frequencies with the gear mesh frequencies and its multiples indicated that the CH-47 housing would react as a forced-response vibration, i.e. no amplification due to resonances, and the UH-1D housing would react as a resonant-response vibration. The reason given was that most of the gear mesh frequencies for the CH-47 geared transmission were lower than the fundamental

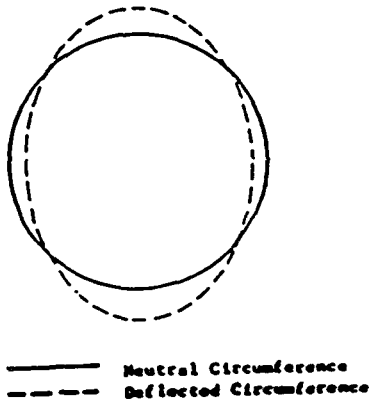

Figure 22. Circumferential mode shape (n=2) [13,15]

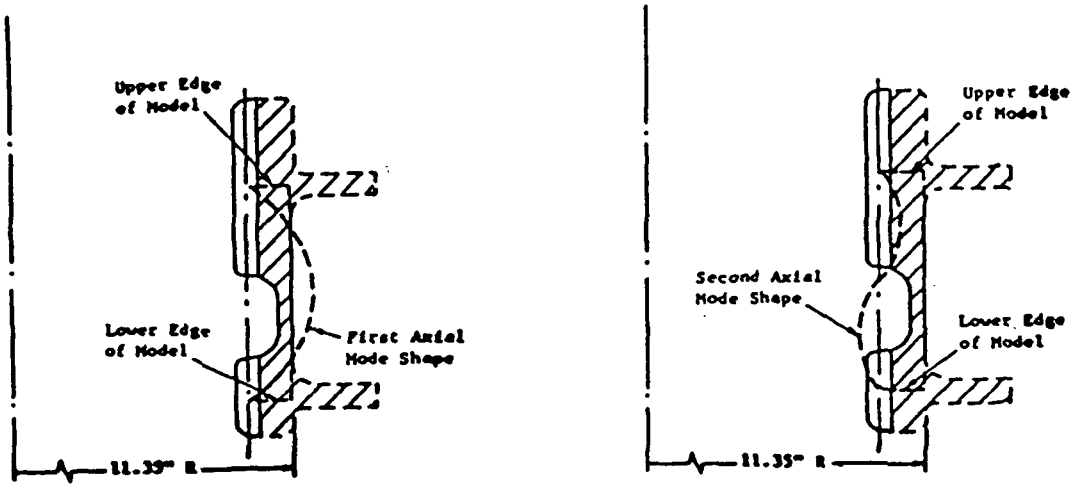

First Mode

Second Mode

Figure 23. First and second axial mode shape [13,15]

Table 2. Natural frequencies (Hz) of the CH-47 and UH-1D gear housing [13,15]

Circumferential	First Axial Mode		Second Axial Mode	
Wave Number n	CH-47	UH-1D	CH-47	UH-1D
0	4350	4380	13500	5470
4	5220	4020	14300	5370
6	6350	3960	15450	5440
8	7660	5800	16500	7500
12	10950	9450	19800	--

natural frequency of the housing, whereas a number of the gear mesh frequencies for the UH-1D geared transmission is very close to the first axial with second and fourth circumferential modes.

In the forced vibration analysis, the dynamic tooth loads obtained by Laskin, Orcutt and Shipley [9,10] discussed in section B, were expressed as a Fourier series and used as the input to this analysis. This exercise could be shown by considering the dynamic tooth loads of the form [9]

$$F_A(\theta, t) = F_A(\theta) \cos \omega t \tag{16}$$

where $F_A(\theta)$ = circumferential distribution of radial forces
ω = forcing frequency (rad / sec)
t = time
θ = angular position with respect to gear A (Figure 24)

Figure 24 illustrates the coordinates of the planetary gear system. Expansion of the function representing the circumferential distribution of the radial forces, as shown in Figure 25, as

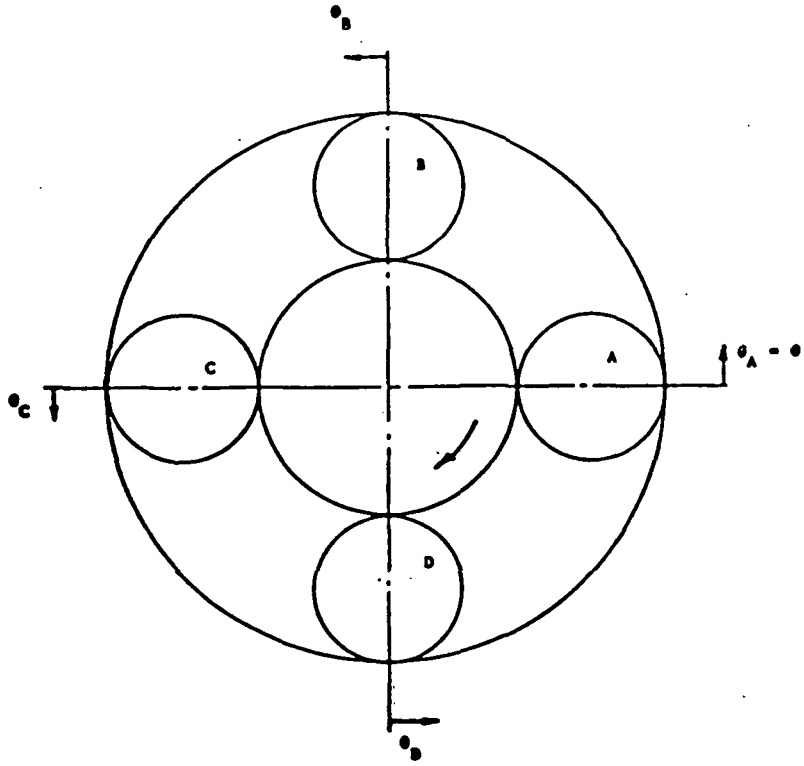

Figure 24. Schematic diagram and the coordinate system for the UH-1D lower planetary gears [9]

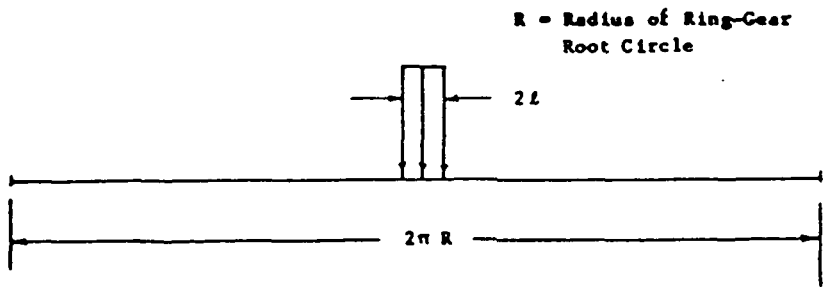

Figure 25. Circumferential distribution of the radial force of one planet gear [9]

a Fourier series led to [9]

$$F_A(\theta) = \frac{a_0}{2} + \sum_1^\infty a_m \cos m\theta \tag{17}$$

where a_0 and a_m are the Fourier coefficients. Equation (16) and (17) were used to characterize the forcing function due to planet gear A. The dynamic response of the gear housing for each Fourier coefficients were then computed, and the form of the response function may be written as [9]

$$w(\theta_A, z, t) = b_A(\theta_A, z) \cos \omega t \tag{18}$$

Finally, the responses due to planet gear B, C and D were obtained in a similar fashion. Using the method of superposition, the total response was constructed by the addition of each responses using the appropriate spatial and temporal relationships. Responses of the two transmission, shown in Figure 26 and 27, were found to support the prediction that the

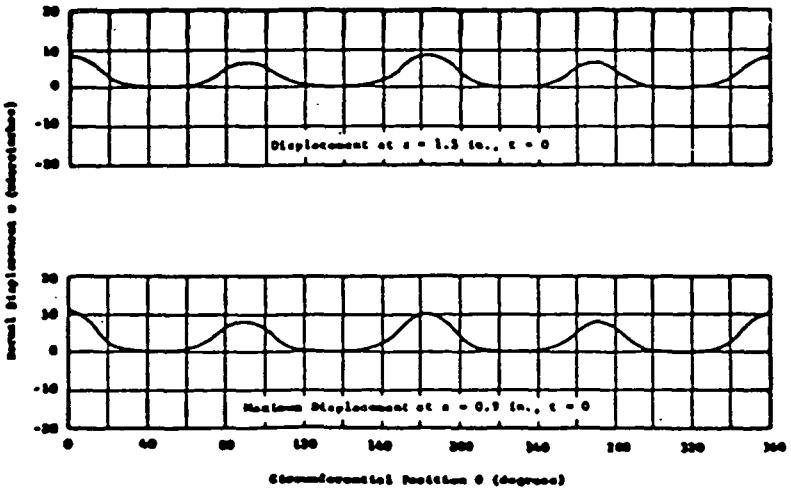

Figure 26. Normal displacement of the CH-47 housing due to lower planet gear forces [9]

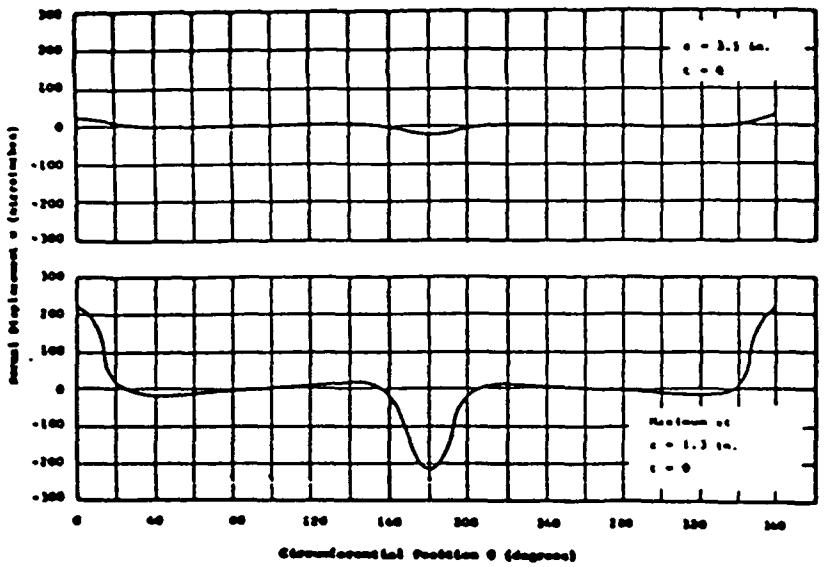

Figure 27. Normal displacement of the UH-1D housing due to lower planet gear forces [9]

CH-47 ring gear housing acted as a vibration energy transfer (forced-response) while the UH-1D one acted as a noise source (resonant-response).

With respect to earlier coupled housing and gear-shaft vibrations model, Astridge and Salzer [24], in 1977, used the semi lumped-mass approach (the stiffness matrix of the complex housing section was obtained using FEM) to model the Wessex Tail Rotor gearbox shown in Figure 7. Out of the 13 lumped-mass locations specified as mentioned before, each with 6 degrees of freedom, 6 of them are located at the housing structure. Although the transmission is quite complex, a simple model was chosen to incorporate the dynamics of the gear-shaft and housing into one single model.

Some experimental methods such as operating motion survey [42,45], and experimental modal analysis [32,45,46] were also used to model the vibrational characteristics of the gear housing plates and to obtain its system parameters. The advantage of using these methods as compared to the purely analytical method is that the system matrices are constructed from a response data of a real gearbox, where else the

development of an analytical model requires knowledge of the housing dynamic behavior and assumptions to simplify modeling procedure.

The operating motion survey technique involves extraction of the mode shapes and natural frequencies by examining the transfer function between 2 points on the gear housing. Since this method requires mounting of at least two acceleration measuring devices (accelerometers), these devices may alter the system characteristics. Singh, Zaremsky, and Houser [45] used this method in addition to structural modal analysis and acoustic intensity methods to correlate gear housing plate natural frequencies to their mode shapes. The comparison of the second mode shapes using these methods is shown in Figure 28a, 28b and 28c.

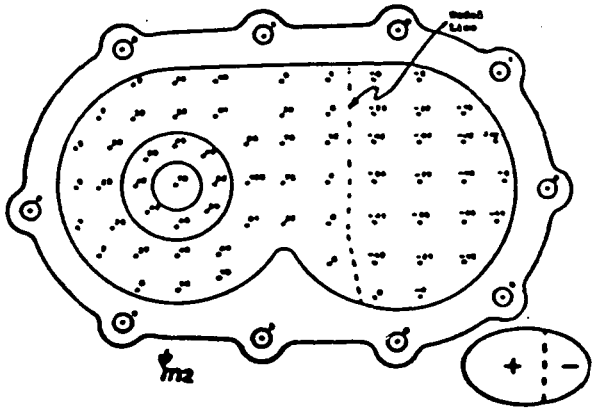

Figure 28a. Normalized contours of the 2nd mode (modal analysis) [45]

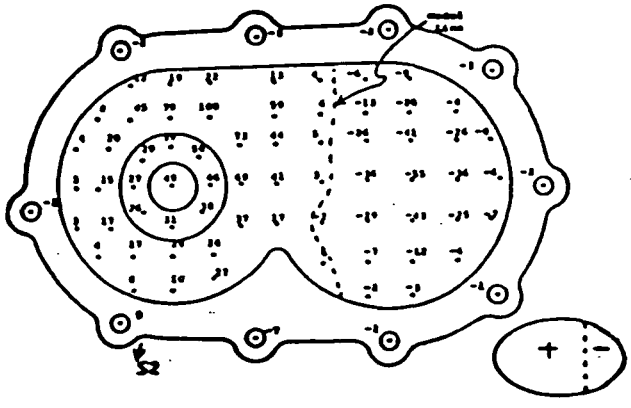

Figure 28b. Normalized contours of the 2nd mode (operating motion survey) [45]

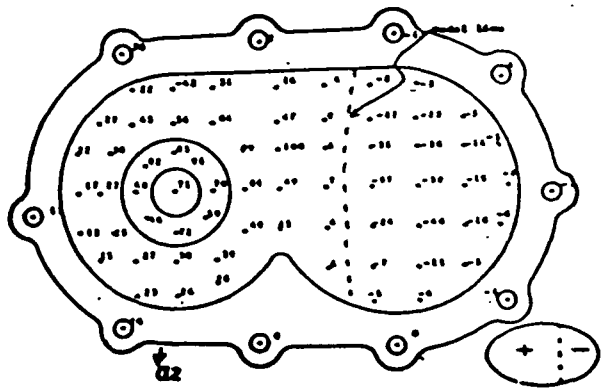

Figure 28c. Normalized acoustics intensity contours of the 2nd mode [45]

The experimental modal analysis technique has also been widely used not only in dynamic analysis of gearbox but also in many other mechanical systems. Modal analysis may be defined as the characterization of the dynamic properties of an elastic structure through the identification of its mode shapes and natural frequencies. The general steps involve are measurements of force and response signal, determination of frequency response function using Fourier Transform, and curve fitting to obtain natural frequencies, damping, and transmissibility from one point to another. This method allows one to obtain the modes of vibration by avoiding interference from the excitation frequencies. As mentioned before, Singh, Zaremsky and Houser [45] used this method to obtain inertance transfer function of 75 locations for the housing plate shown in Figure 28. Van Haven, De Wachte and Vanhonacke [46] also used the experimental modal analysis technique to characterize a gear-motor housing reported to radiate excessive noise. They claimed that the fundamental frequency coincided with one of the gear mesh frequency, and by ribbing the housing interior shifted the natural frequency away from the excitation frequency.

Rajab [32] also used experimental modal analysis to model a clamped plate with one support bearing on it as shown in Figure 14 of section B. This model together with the shaft and bearing models were combined using the building-block system (substructure

type) analysis where the total system dynamic matrix is constructed from the individual component dynamic matrices. This resultant system matrix equation was used for forced response analysis to optimize the bearing location for reduced transverse plate vibration.

With some advancement in acoustic intensity measurement technique recently, Singh, Zaremsky and Houser [45]was able to use this method to perform "in-situ" measurements of acoustic intensity very close (0.5 in.) to the surface of the vibrating housing plate shown in Figure 28. The two-microphone cross-spectrum technique was actually used to obtain the housing plate vibration modes which were found to compare well with other methods such as modal analysis and operating motion survey as shown in Figure 28. The acoustic intensity very near the surface was estimated to be [45]

$$\vec{I}_r = \langle p u_r \rangle_t \tag{19}$$

where

$$p = \frac{p_1 + p_2}{2}$$

$$u_r = \frac{-1}{\rho_o} \int \frac{p_1 - p_2}{\Delta} \, dt$$

with

p = sound pressure
u_r = radial velocity
ρ_o = air density
Δ = microphone spacing
$\langle \rangle_t$ = time averaged

and where the accuracy depended on the microphone spacing Δ, and the proximity to the radiating surface.

Bowes, et. al. [17-19], in 1977, as mentioned before in the previous section included the effects of housing mass, stiffness, and damping in the gearbox noise and vibration

analysis of the SH-2D helicopter transmission. Component synthesis method was used to connect the gear-shaft system with the gear housing system. This was done by summing the terms in the subsystem impedance matrices which corresponded to the same global position. The method used to derived the housing impedance was an incomplete modeling technique using modal data and approximate mass matrix. The housing was suspended using a low rate stiffness to isolate it from its environment for modal testing. Initially, the housing was divided into many elemental masses with its corresponding degree of freedom. Bowes, et. al. [17-19] used 44 housing degrees of freedom on the SH-2D housing where 20 of which corresponded to the interface degrees of freedom. Then the diagonal mass elements were obtained from the elemental masses while the off-diagonal elements were estimated. The new modified mass matrix was obtained from the approximate matrix by imposing the condition [19]

$$\{\phi_i\}^T [M] \{\phi_j\} = 0 \quad , \text{ for } i \neq j \tag{20}$$

where $\{\phi_i\}^T$ = transpose of i-th normal mode

$[M]$ = mass matrix

$\{\phi_j\}$ = j-th normal mode

In addition, the matrix containing stiffness and damping was computed using [19]

$$[K] = [M]\left(\sum_{1}^{N} \frac{\Omega_i^2}{m_i} \{1 + jc_i\} \phi_i \phi_i^T\right)[M] \tag{21}$$

where Ω_i = i – th natural frequency

c_i = i – th damping coefficient

$j = \sqrt{-1}$

The undamped impedance matrix was then obtained from the mass and stiffness matrices [19]

$$[z] = -\omega^2 [M] + [K] \tag{22}$$

which will be used with the gear-shaft system impedance matrix to analyze the gearbox dynamics.

The finite element method (FEM) was also widely used due the existence of general purpose finite element program such as NASTRAN, ISAP-4, SPADAS, ANSYS, etc. In most cases, the gear housing was modeled independently from the geared transmission with assumed boundary conditions and/or input dynamic bearing/gear forces at the interfaces. Kato, Takatsu and Tobe [42] used 480 plate elements on ISAP-4 to obtain the vibration modes of a simple gear housing consist of rectangular plates. An example of a mode shape computed is shown in Figure 29.

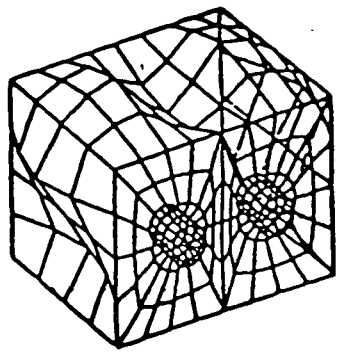

Figure 29. Vibration mode of a gear housing (0.4m x 0.32m x 0.28m) at 1320 Hz [42]

Croker, Lalor and Petyt [47] used isotropic thin flat plate and isoparametric thick flat plate elements ,shown in Figure 30, on SPADAS to model the vibration of an engine block.

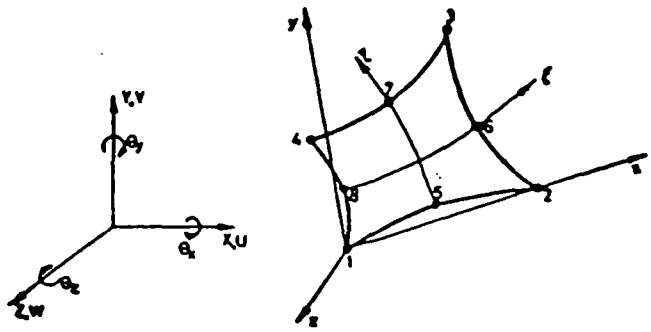

Figure 30. Isoparametric thick flat plate element (8 nodes, 6 DOF/node) [47]

Substructure method which involve dividing the housing into several parts resulting in smaller mass/stiffness matrices and assembling the global matrices with the assumption that each substructure can be adequately represented by only a few modes. Using the properties of symmetric and antisymmetric motions, the model size was reduced, but two separate analysis were done instead. For example [47], a symmetry about the y-z plane would require

$$u = \theta_Y = \theta_Z = 0 \tag{23}$$

while an antisymmetric motion about y-z plane would require [47]

$$v = w = \theta_X = 0 \tag{24}$$

where u, v, w = displacement in the x, y, z – directions
$\theta_X, \theta_Y, \theta_Z$ = rotation about the x, y, z – axis

A typical correlation between the theoretical and experimental natural frequencies is shown in Figure 31.

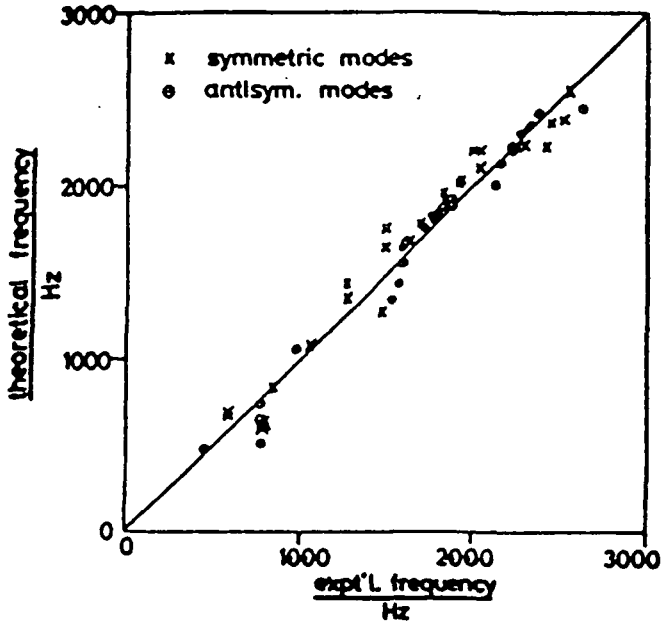

Figure 31. Correlation of theoretical and experimental natural frequencies [47]

In the effort to model the complex CH-47 helicopter transmission housing, Drago, et. al [4,8,28,29,48] used the NASTRAN finite element program to develop 3 complex finite element models of the CH-47 gear housing parts. The models are for the upper cover, ring gear housing, and case as shown in Figure 32. Quadrilateral and triangular homogeneous plate elements with membrane and bending capabilities. The 3 sections were analyzed separately with simply supported boundary conditions at the interfaces to simulate restraint on the boundaries by adjacent sections. Table 3 list some of the natural frequencies of each section which are in the vicinity of the planetary gear mesh frequencies.

Strain energy methods was also used with the above finite element models to calculate the strain energy density for each troubled vibration mode. The structural elements with the highest strain energy per unit volume were determined as the best choice for structural modification. This local alteration of the housing would require minimal weight change for

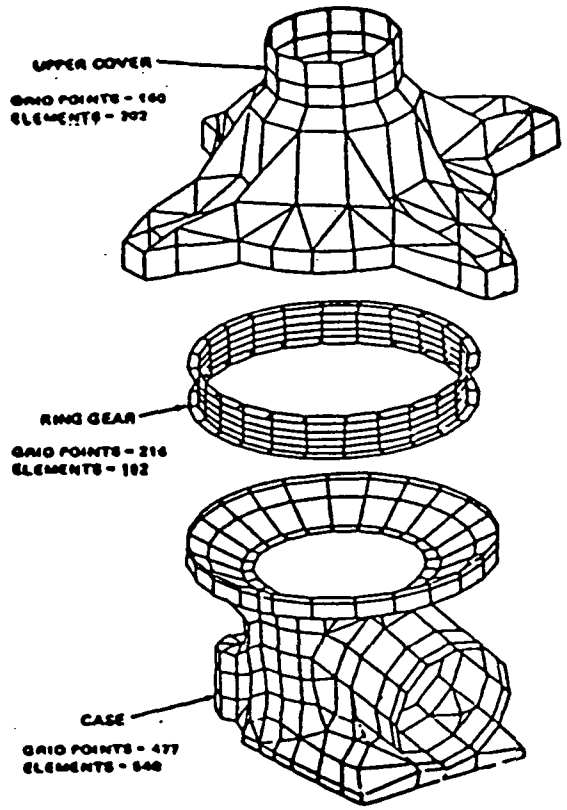

Figure 32. Finite element housing transmission model for CH-47 [8]

maximum shift in the natural frequency. Areas of high strain energy for modes 3 and 4 are shown in Figure 33.

Finally, the statistical energy approach in characterizing the dynamic behavior of the gear housing by statistical means was used by Lu, Rockwood and Warner [34] as discussed in detail in the previous section. They summarized that this method is suitable for average response determination in the high frequency range. On the other hand, finite element method was recommended for estimating the response at the lower frequency range due to the detail information available.

Table 3. Some of the natural frequencies near the excitation frequencies [48]

Excitation Frequencies	Calculated Natural frequencies (Hz)		
	Upper Cover	Gear Housing	Case
1566	1518	--	1541
	1568	2334	1603
3132	3069	2565	3103
	3133	3206	3181
3606	3570	3206	3588
	3653	4130	3664
4698	4577	4130	4667
	4775	4770	4735

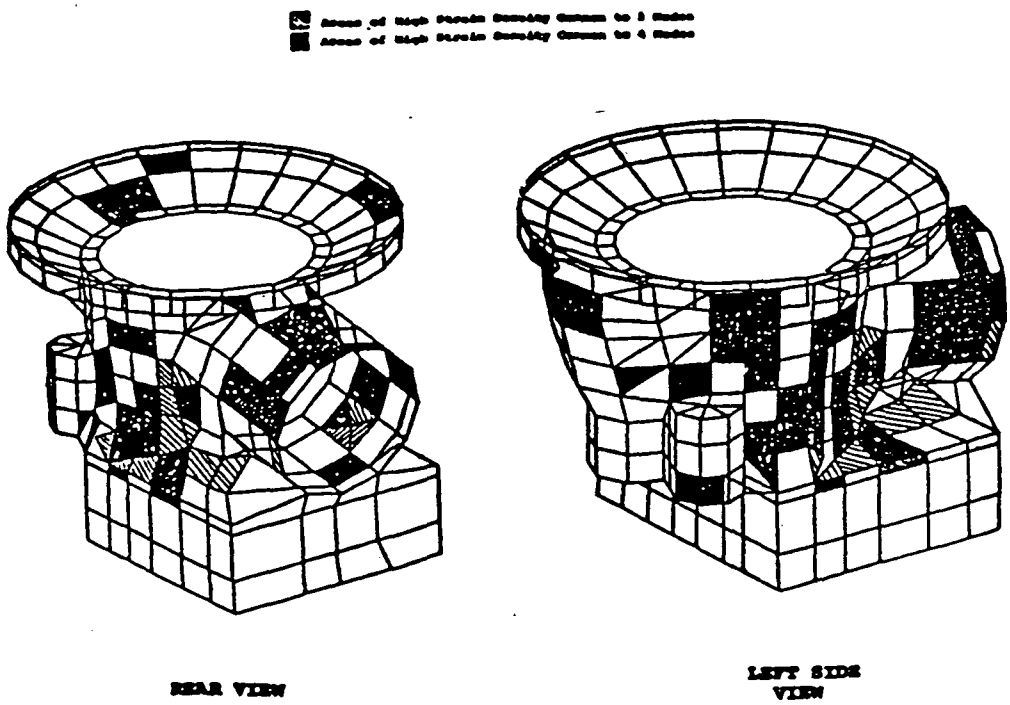

Figure 33. Areas of high strain energy density for modes 3 and 4 [8]

D. Noise Radiation [4,7,9-15,17-19,22,23,26,35,38,39,41,42,44,45,49-59]

Gearbox noise radiation model has been semi-empirical in nature due to the complexity of the interactions between a vibrating gearbox structure, such as a gear housing and its surrounding fluid. Exact mathematical solution to a sound radiating surface in oscillatory motion has been restricted to simple sound sources and highly idealized environment, such as a pulsating or oscillating sphere and piston radiator [7]. There were many attempts in the past to characterize and correlate gearbox noise frequency spectra with the structural vibration and/or excitations spectra using semi-empirical prediction formulas and various experimental technique [4,11,13-15,18,19,26,35,38,39,42,44,45,49,50]. Most have concluded that the noise prediction is quite complicated and hence an analysis requires many assumptions.

Laskin, Orcutt and Shipley [9,10], in 1968, related the vibration energy in the gearbox to noise radiated. They derived a gearbox noise level mathematical expression by establishing a semi-empirical relationship between the acoustic energy and gear excitation energy. To show this, the total vibration energy E_M generated by the gear excitations was formulated by Laskin, et. al.[9], as

$$E_M = \left(\frac{\delta_0 F_0}{4}\right) \{ -\cos(2\omega t + \theta) + 2\omega t \cdot \sin(\theta) \} \qquad (25)$$

where

δ_0 = excitation amplitude
F_0 = force amplitude
θ = phase angle
$\omega = 2\pi f$ = frequency of vibration (rad / sec)

The first term on the right hand side of equation (25) represented mechanical vibration energy, whereas the second term represented dissipated energy through structural dampings. The acoustic energy released per cycle E_A [9],

$$E_A = \alpha \frac{\delta_0 F_0}{4} \tag{26}$$

was then obtained by introducing an energy conversion factor (acoustic efficiency) α for the mechanical energy part. By summing all excitations which contributed to the noise level at frequency f, the sound power W_A expression became [9]

$$W_A = \frac{1}{2}\alpha f \sum \delta_0 F_0 \tag{27}$$

Equation (27) was also expressed in sound pressure L_P, dB at distance r by referencing it to a standard set of conditions (point source, free-field, atmospheric temperature=68^{o}F and pressure=29.5 in-Hg) and introducing geometry and environment factor β. The sound pressure level L_P was given as [9]

$$L_p = 10 \log \left[\frac{\rho_o c_o \, \alpha \beta f \sum \delta_0 F_0}{8 \pi r^2 p_o^2} \right] \tag{28}$$

where the reference pressure is $p_0 = 2 \times 10^{-5}$ Pa and the acoustic impedance is $\rho_0 c_0 = 473$ kg / m^{2}s. It was noted that the accuracy of this formula depended on the value of the two factors, i.e. α and β, in equation (28). Badgley and Laskin [11], in 1970, rewrote the above sound pressure level expression at third-octave band widths and at full-octave band widths by introducing a filter attenuation factor at each band width.These semi-

empirical relationships were found to predict poorly when compared to experimental data as shown in Figure 34 due to the reason mentioned before, that is the uncertainty in the numerical values of the factors involved. However, it was noted from the same figure that the character of the noise level is similar to the measured level if the amplitude difference is ignored.

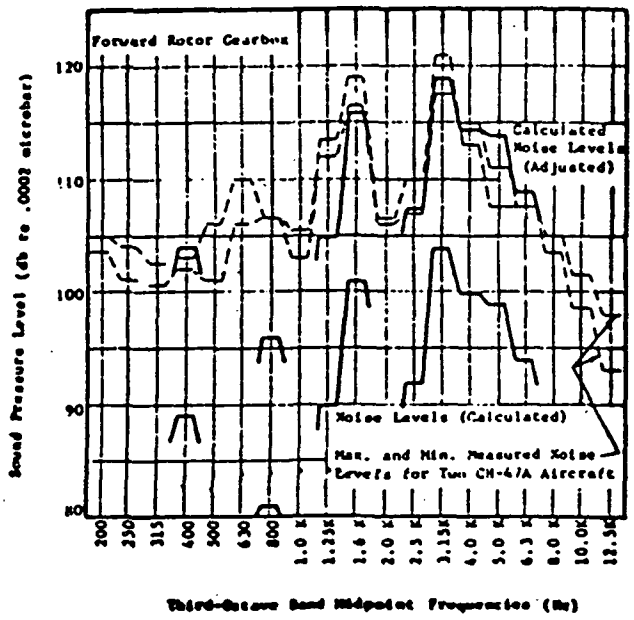

Figure 34. Comparison of empirically prediction gearbox noise and experimental data for cruise flight condition (CH-47 helicopter) [11]

Badgley and Chiang [12,-14], in 1972, estimated the sound power radiated W_A by the CH-47 ring gear housing using a semi-empirical formula, based on a point source assumption and unity radiation efficiency, given below as [12]

$$W_A = \omega^2 w^2 A \rho_o c_o \tag{29}$$

where w = averaged normal displacement of housing

ω = frequency (rad/sec)

A = Area

c_0 = sound velocity

ρ_0 = density of medium

The computation of the ring gear housing average displacement was obtained from a composite cylindrical shell structure model of the ring gear housing discussed in section C. A shortcoming of this formula is no inclusion of the housing geometry. In addition they also expressed the equivalent noise level change L_{eq},dB as [14]

$$L_{eq}(dB) = 20 \log \frac{\sum F_B^{\,N}}{\sum F_B^{\,0}} \tag{30}$$

where $F_B^{\,0}$ and $F_B^{\,N}$ are the original and new bearing forces respectively. This changes allowed them to evaluate modifications in the geared system design using bearing forces for reduced noise level. Similarly, Salzer, Smith and Welbourn [22,23] assumed that the housing does not change the noise character, and used the bearing force frequency spectra to represent the noise in their analysis.

Section B of this review mentioned Bowes, et. al. [17-19] refined Badgley and Chiang models of geared transmission system. In the process, Bowes, et. al. [19] modeled the gear housing as a small number of simple, baffled, hemispherical acoustic sources. Each source size was estimated as [19]

$$s_i = \sqrt{\frac{R_o^{\,2}}{n}} \tag{31}$$

where s_i = hemispherical source radius

R_0 = radius of sphere enclosing transmission housing

n = number of sources

Hence based on this assumption, the total sound power radiated (summation of all the sources) was computed using [19]

$$W_A = \sum_1^n \left[\frac{s_i^4 (a_0)_i^2 \rho_o c_k^2 \pi}{\omega^2 (1 + k^2 s_i^2)} \right] \tag{32}$$

where $(a_0)_i$ = absolute amplitude of acceleration at point i

k = wave number

c_k = speed of sound

ρ_o = medium density

A typical comparison between the theoretical prediction and experimental data is shown in Figure 35. Within each frequency band, the prediction closely match the experimental data.

Ishida, Matsuda and Fukui [35], on the other hand modeled an automobile gear housing as a circular piston in an infinite baffle to obtain relationship between the sound pressure p and acceleration or velocity of surface vibration. He summarized these relationship as [35]

$$p \propto \omega^2 x \quad \text{when } ka<2 \qquad \text{or,} \qquad p \propto \omega x \quad \text{when } ka>2 \tag{33}$$

where x = amplitude of surface vibration (displacement)

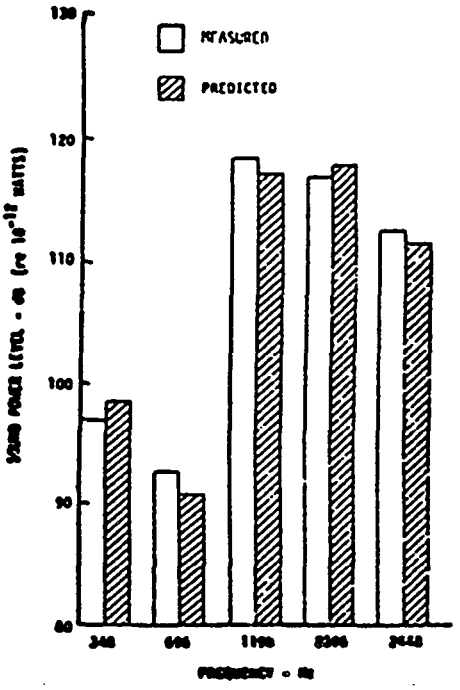

Figure 35. Theoretically and experimentally determined sound pressure level [19]

k = wave number

a = radius of the circular piston

$\omega^2 x$ = acceleration of vibration

ωx = velocity of vibration

Hence, the sound pressure level would be either proportional to the acceleration or velocity level depending on the area of the vibrating surface.

The link (radiation efficiency) between the structural vibrations and sound pressure level assuming an ideal environment is the most important steps in predicting noise from a vibrating surface. It is also very difficult to estimate due to the complexity of the noise

generating mechanisms and the fluid-structural interactions, as mentioned earlier. Except in very simple cases [51-54], the analytical expression for the radiation efficiency, defined below [52], is generally not available. The radiation efficiency σ_{rad} is

$$\sigma_{rad} = \frac{P_A}{\rho_0 c_0 S \langle v \rangle_{s.t.}^2} \tag{34}$$

where P_A = sound power

S = vibrating surface area

$\langle v \rangle_{s.t.}$ =mean rms surface velocity (spatially averaged)

c_0 = sound speed of the medium

ρ_0 = medium density

Richard [55] realized the elaborate computation and difficulty that one might encounter in noise prediction, offered an expression for the A-weighted equivalent sound pressure level (db) in terms of structural response, radiation efficiency, damping, machine bulkiness etc. given by [55]

$$L_{A,eq}(f) = 10 \log E_{escape} + 10 \log(s.c.) + 10\left(\frac{A \sigma_{rad}}{f}\right) - 10 \log \eta_s - 10 \log d + B \tag{35}$$

where $L_{A,eq}$ = A-weighted equivalent sound pressure level

E_{escape} = total structural energy

s.c. = fraction of E_{escape} in the frequency band of interest

A = A-weighted correction

σ_{rad} = radiation efficiency

f = frequency (Hz)

η_s = damping

d = machine bulkiness

B =constant

This formula do not give exact noise level but does indicate the probable factors that might explain high noise level in a particular machinery, in this case a gearbox. The contribution of each factor to L_{eq} in graphical form is shown in Figure 36.

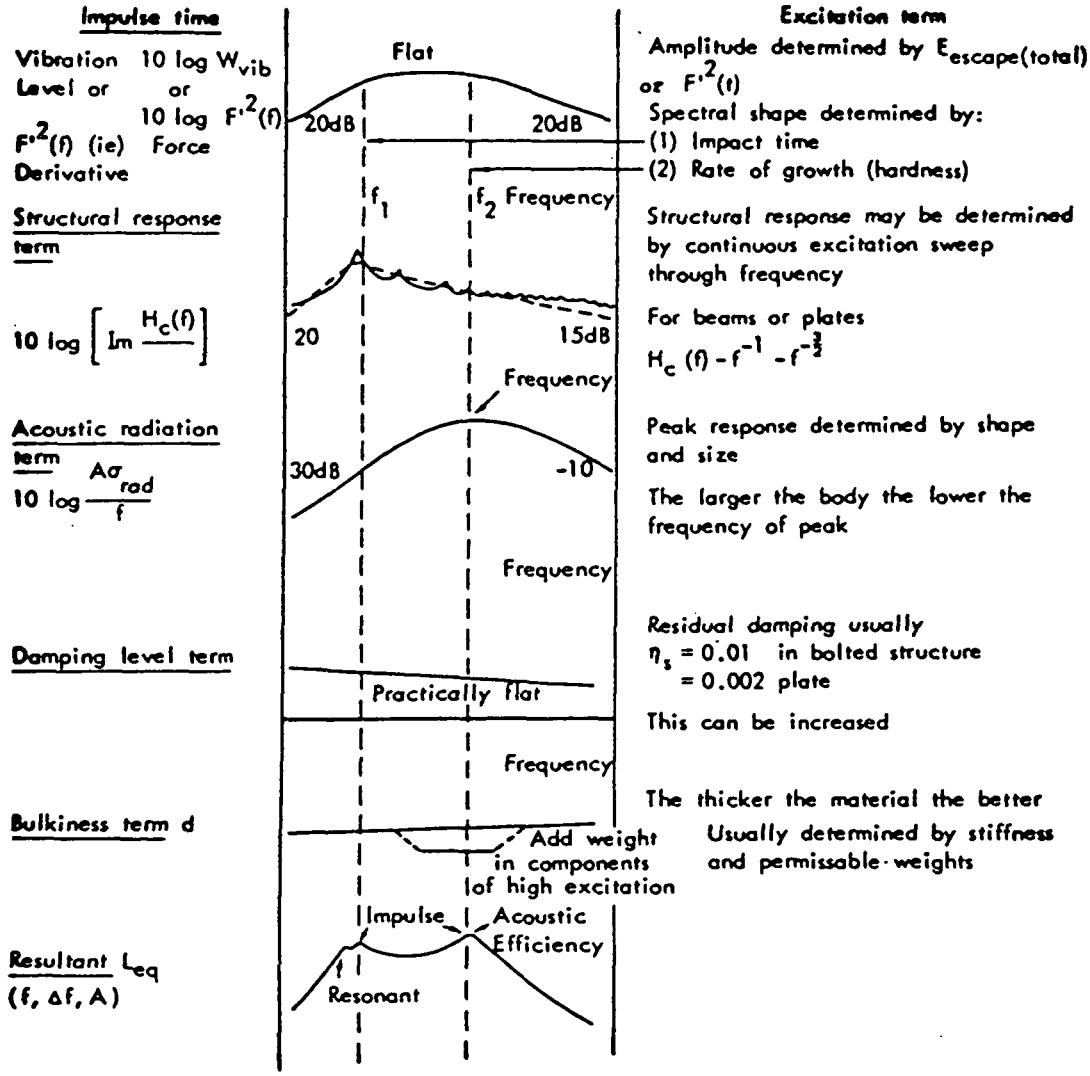

Figure 36. Total noise level in a machinery noise application due to various factors [55]

Although gearbox noise prediction models has been mostly semi-empirical, there exist some numerical methods like the finite element method, finite difference method, and boundary element method for noise prediction. These methods are usually difficult to apply for complex geometry, and therefore has not been used in gearbox noise analysis. The finite element method requires three dimensional acoustic finite element model to characterize the noise field exterior to the structure. In addition, there is the problem of the termination location for this model which in reality is at infinity for free field condition. Therefore, this method is used primarily for closed spaces, and low frequency due to the fact that the nodal points spacing must be less than a quarter wavelenght. Finite difference method has also similar problem too. Boundary element method [56,57] has been more popular because it involves solution to a two dimensional problem of the Helmholtz integral equation. It is most suitable for free field sound radiation computation. This method requires knowledge of the structural vibration modes which can be obtained using a finite element method or an experimental modal analysis. The Helmholtz integral equation is given by [56]

$$C(y)\,P(y) = \int_S \left[P(Q)\,G'(P,Q) + iz_0 k\,v(Q)\,G(P,Q)\right] dS(Q) \qquad (36)$$

where

Q = surface point

y = point exterior to the structure

P = acoustic pressure

$$C = \begin{cases} 2\pi \text{ if } y \text{ on surface} \\ 4\pi \text{ if } y \text{ exterior of surface} \end{cases}$$

z_0 = characteristic impedance

k = wave number

G = exp (-ikR) / R (Green's function)

()'= normal gradient

v = surface velocity

The above equation are then reduced to a set of algebraic equation by discretizing the noise radiating surface with appropriate elements. These equations will relate normally the surface acoustic pressure to the structural surface velocity.

Few experimental methods such as acoustic intensity method [42,45,52], free field measurement technique [12,35,49-51,58,59] and acoustical holography method [42,59] were also used widely to characterize gearbox noise level due to the many difficulties involved in applying the above methods practically. Free field measurement technique requires an anechoic environment whereas the acoustic intensity method allows "in-situ" tests. The basis for computing the intensity using this method is given in equation (19) of section C. Singh, Zaremsky and Houser [45] used the two microphone "in-situ" acoustic intensity method obtain sound intensity very close to the surface of a gear housing plate also discussed in section C of this review. Kato [42] performed "in-situ" acoustic intensity measurements on gearbox noise in poor acoustical environment. The results indicated that certain intensity components intensified by 2 dB (small error) when measurements were made near reflecting walls. The explanation given was the diffraction of the sound waves occurring. An example of the intensity distribution on the measurement surface around a simple 0.4m x 0.32m x 0.28m gear housing is shown in Figure 37. Janssen and De Wachter [52] also used intensity method to evaluate the contribution of partial surfaces of a housing to the total noise radiated. The information was used to aid in design changes by use of blocking mass to reduce noise level. Umezawa and Houjoh [59] has developed an acoustical holographic system to show locations of sound sources in machinery. The process involved hologram recording, reconstruction of recorded wavefront, and intensity distribution calculation. This method was applied to an operating simple gearbox. The

results obtained were fundamentally known such as the frequency content, noise source, etc.

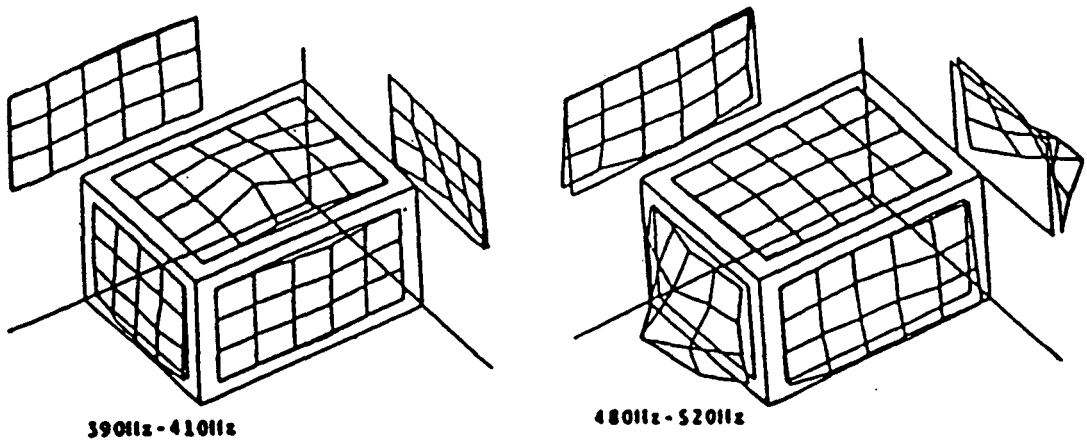

Figure 37. Intensity distribution around the simple gearbox obtained using acoustic intensity method [42]

E. Gearbox Mount System [7,13,51,60-66]

Basic theory on vibration isolation of simple vibrating system, such as the one degree of freedom mass-spring-damper system, has been rigorously treated. The reader is referred to references [51,60,61] or other equivalent texts for more information. Here, the mounts and suspensions of gearbox will be discussed. As mentioned previously that the gear excitations not only caused gear housing vibration and noise radiation but the vibrational energy may also be transmitted through the mounts and suspensions to structures attached. In addition, there will dynamic interactions between the gearbox mounts and gear housing which cannot be ignored.

One of the earlier attempt to model the helicopter gearbox mounts and suspensions was done by Badgley and Chiang [13], in 1972. The model consisted of the gearbox mount, isolators, the aircraft structure using combination of mass, linear spring, and linear dampers as shown in Figure 38. The isolators was assumed to be massless which resulted

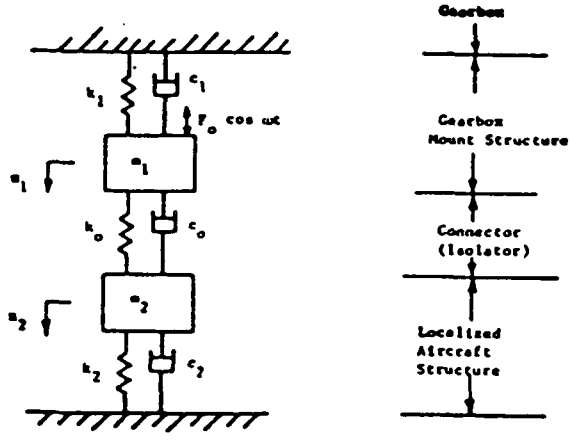

Figure 38. Analytical model for the gearbox to airframe isolators [13]

in only two degrees of freedom system. The vibration source was applied at the gearbox mount and was assumed to be oscillatory. Using standard method, the equation of motion derived was [13]

$$m_1\ddot{x}_1 + c_0(\dot{x}_1 - \dot{x}_2) + c_1\dot{x}_1 + k_0(x_1 - x_2) + k_1x_1 = F_0 \cos\ \omega t \qquad (37)$$

$$m_2\ddot{x}_2 + c_0(\dot{x}_2 - \dot{x}_1) + c_2\dot{x}_2 + k_0(x_2 - x_1) + k_2x_2 = 0 \qquad (38)$$

where the symbols are defined in Figure 38. Then the force and motion transmissibilities, T_m and T_f respectively, was obtained as [13]

$$T_m = \frac{|z_0|}{|z_0 + z_2|} \qquad (39)$$

$$T_f = \frac{|z_0\, z_2|}{|z_1\, z_2 + z_0\, z_1 + z_0\, z_2|} \qquad (40)$$

where
$$z_0 = c_0 - i\frac{k_0}{\omega} \quad \text{(mechanical impedance of isolator)}$$
$$z_1 = c_1 + i\left(m_1\omega - \frac{k_1}{\omega}\right) \quad \text{(mechanical impedance of mount)}$$
$$z_2 = c_2 + i\left(m_2\omega - \frac{k_2}{\omega}\right) \quad \text{(mechanical impedance of aircraft)}$$

Based on this simple analysis, Badgley and Chiang [13] concluded that for low motion and force transmissibility, the mechanical impedance of the isolator must be small, and the mechanical impedances of the local gearbox mount and local aircraft structures must be high. In other words, the isolator must be made as soft as possible with low damping, while the gearbox mount and aircraft structures must be massive and highly damped. The

difficulty in obtaining reliable physical values like mass, spring, and damping was also mentioned. Several methods were suggested, that is, numerically compute these physical quantities based on the geometry and material, and experimentally extract the impedances.

Warner and Wright [62], and Andrews [63] investigated various marine gearbox mounts and isolators requirements for reduction in the force/motion transmissibilities. These studies have resulted in the design of special purpose isolation system. Warner and Wright [62] identified the energy source such as the transmission error at mesh frequency and unbalance of gears and shafts contributing to the vibration transferred through the marine gearbox mounts. The addition of damping at the isolators was recommended to damp the rigid body modes which might amplify the unbalance vibration of the gear-shaft system, although it may reduce the effectiveness of the isolators. Based on these observations, a metallic isolation system, shown in Figure 39 was recommended.

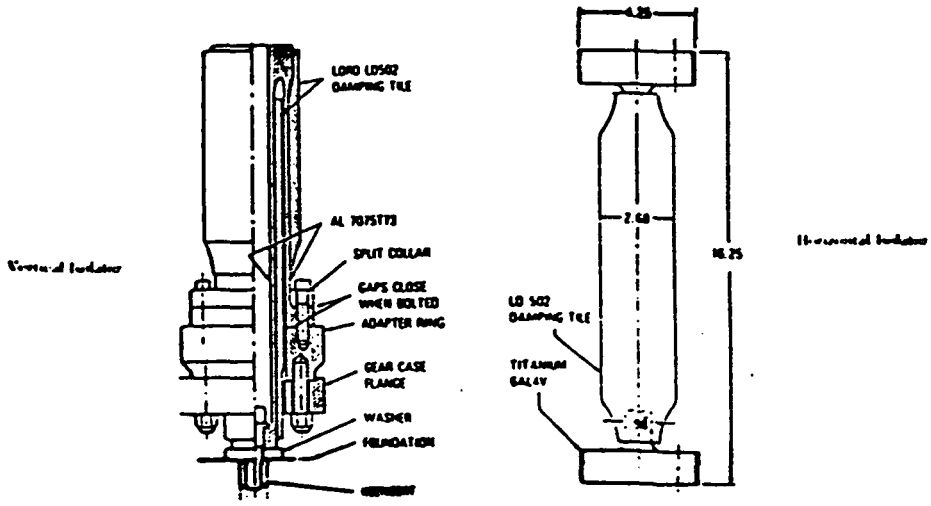

Figure 39. Vertical and horizontal metallic isolator [62]

The performance of these system was not analyzed analytically but was tested experimentally. Some of the features of this system included high stiffness, absence of creep often occur in elastomeric isolators, compact, etc. Figure 40 indicated results of a

free-free test of the vertical isolator. It can be seen to perform as a vibration isolator at a very wide frequency range. The ability of the isolator to act as a vibration isolator when installed is illustrated in Figure 41. Comparison has been made between the installation of

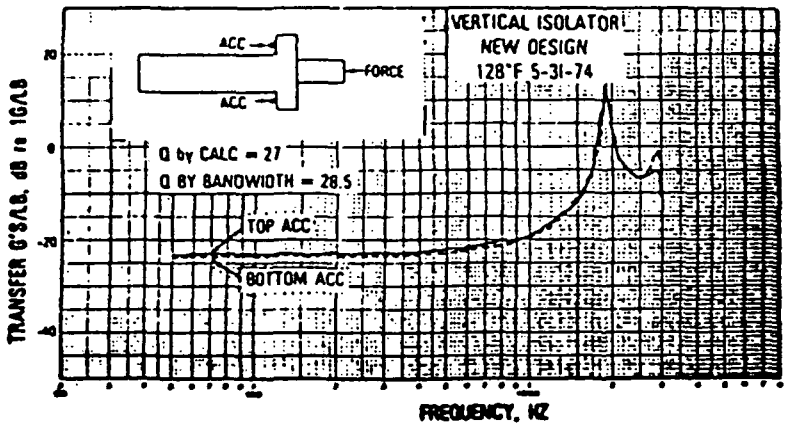

Figure 40. Free-free test of the vertical isolator [62]

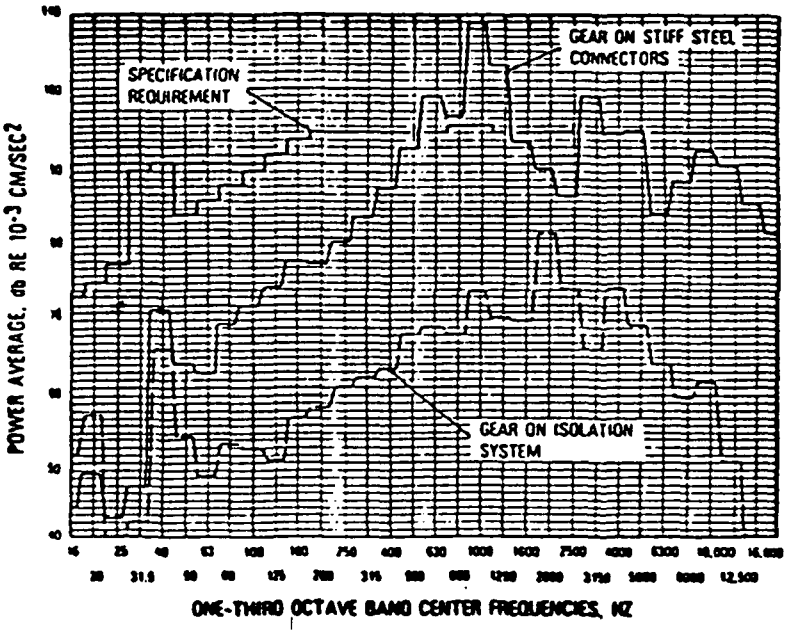

Figure 41. Structure-borne noise at 2680 rpm with various mounting conditions [62]

the stiff steel connectors and the metallic isolation system. Reduction in the structure-borne vibration is observed for the case with the metallic isolators installed.

Andrews [63] utilized the one degree of freedom system isolation concept as a basis for the gearbox mount dynamic model. The gear housing and subbase for the entire system were assumed to be rigid. Only vertical motion was allowed in the mount model and the journal bearing was modeled as linear stiffness. Modal analysis of this system using the model described here indicated that the first two modes were shaft deflection type, and the third and fourth modes were associated with the vertical motion of the mounts. This analysis led to the design of an isolation system shown on Figure 42. The two side rectangular blocks were attached to the gear housing while the middle on to the subbase. Two isolators, one on each side, were required to mount the marine gearbox. Application of this design led to lower gear housing vibration and equality of bearing loads.

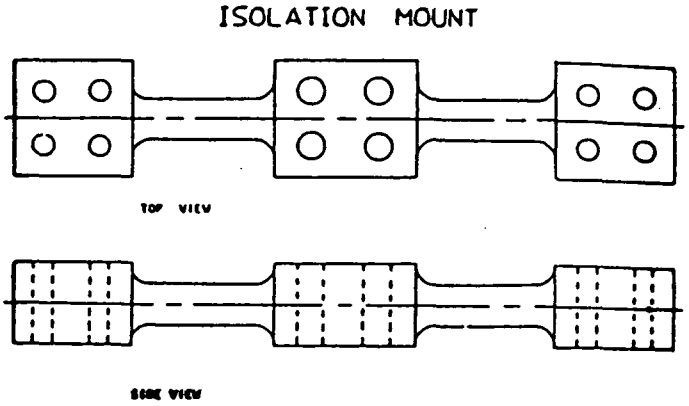

Figure 42. Gearbox isolation system [63]

Snowdon [61] also discussed in detail characteristics of damped discrete and continuous vibration isolators such as elastomeric isolators, combination of spring-damper system isolators, and rods-beams system isolators. The examples were not specifically on

gearbox application but more towards general machinery application. Lunden and Kamph [64] investigated numerically and experimentally the vibration characteristics of a lightweight skeletal machine foundation (grillage) as continuous system isolator. They concluded that by applying "blocking mass" and damping (discrete and distributed) on the system will result in reduction of grillage vibration over a broad frequency interval, and hence lower transmissibility through the grillage system. The damped second order Rayleigh-Timonshenko beam has been used in the numerical studies.

Granhall and Kihlman [65], in 1980, expressed the need for knowing structure-borne sound sources data of a machinery in order to aid in design of mounts and isolators and noise predictions. For this reason, they analyzed a one dimensional vibration isolator system using the mechanical impedances in an analog circuit, and formulated an equation for estimating insertion loss of an isolator from measured impedance data. The insertion loss IL [65] is given by

$$IL = 20 \log \left[\frac{z_f z_i + z_f z_m + z_m z_i}{z_i (z_f + z_m)} \right] \tag{41}$$

where z_m, z_f, and z_i are the internal, foundation, and isolator impedances respectively. If one assumed that the foundation is very rigid, equation (41) may then be written as [65]

$$IL = 20 \log \left[1 + \frac{z_m}{z_i} \right] \tag{42}$$

Comparison of the insertion loss predicted by equation (42) with measured insertion loss data, and the insertion loss of a mass-spring-damper system model is shown in Figure 43 [65]. The graphs indicate that equation (42) predicts the measured data better than the one

predicted by a spring-mass-damper model. However, these results are not found to be true at high frequencies where both models are inapplicable.

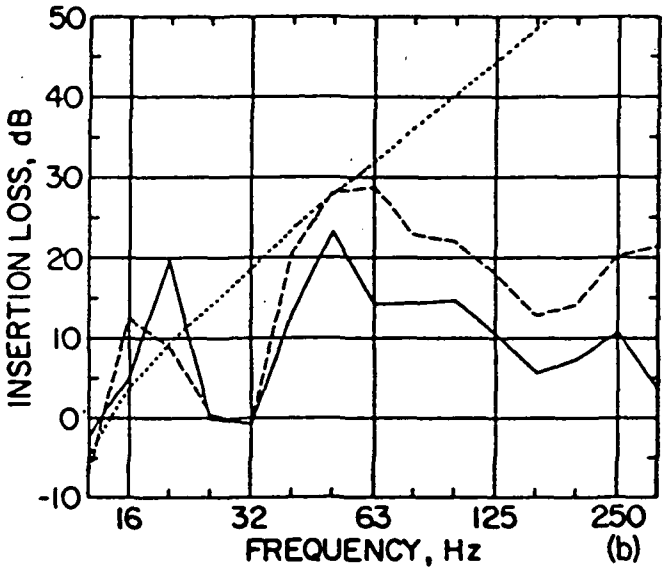

Figure 43. Insertion loss in 1/3 octave bands for a fan unit {solid lines = measured data, dashed lines = equation (42), and dotted lines = mass-spring system}[65]

Unruh [66] developed a finite element dynamic model of an aircraft engine mount to be coupled with the rigid engine model, frequency dependent stiffness model of the isolators, and experimentally obtained fuselage and interior response model. The purpose was to study the effect of isolators and mounts on the structure-borne noise transmission. The vibration isolator modeled as frequency dependent radial k_R and axial k_A springs in local coordinate was given as [66]

$$k_R = k_R^*(\omega)\,[1 + i\eta(\omega)] \tag{43}$$

$$k_A = k_A^*(\omega)\,[1 + i\eta(\omega)] \tag{44}$$

where k_R^* = radial spring modulus amplitude

k_A^* = axial spring modulus amplitude

η = material loss factor

The finite element model of the mount system,illustrated in Figure 44, consisted of 70 elastic beam elements with 201 degrees of freedom. Using modal synthesis method, as

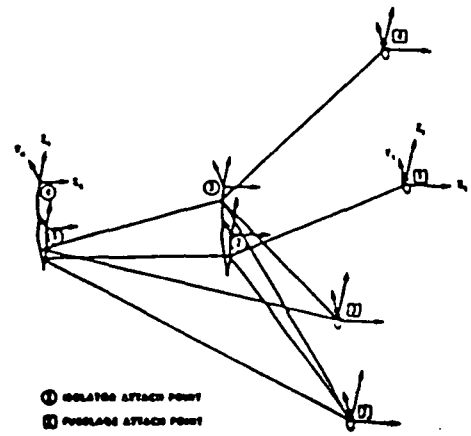

Figure 44. Engine mount structure with coupling degrees of freedom [66]

described in previous section, the number of degree of freedom was reduced to 51 elastic and 6 rigid body degrees of freedom. For each of the subsystem listed above, the standard second order differential governing equation was derived. Then by proper choice of the independent degrees of freedom, each components were coupled together by the summation of interface forces and was set to zero to obtain an empirical relation between the structure-borne noise at various position in the aircraft interior and the chosen degrees of freedom.

Lyon [7] also performed similar analysis on a marine gearbox system schematically shown in Figure 45. This method involved modeling of the gearbox mount system in detail using combinations of simple beam, spring, damper and mass elements. The input and

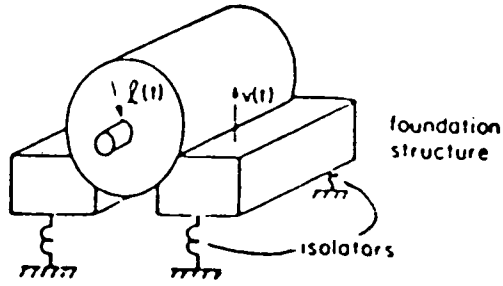

Figure 45. Marine gearbox mounted on a foundation which sits on isolators [7]

transfer impedances of all the elements were assembled into a complete system according to the numbered nodes while setting the total force at each junction equal to zero or to the externally applied force. The impedance of these simple elements can be derived easily. Figure 46 illustrated the model of a reduction gearbox mount system. A set of mass

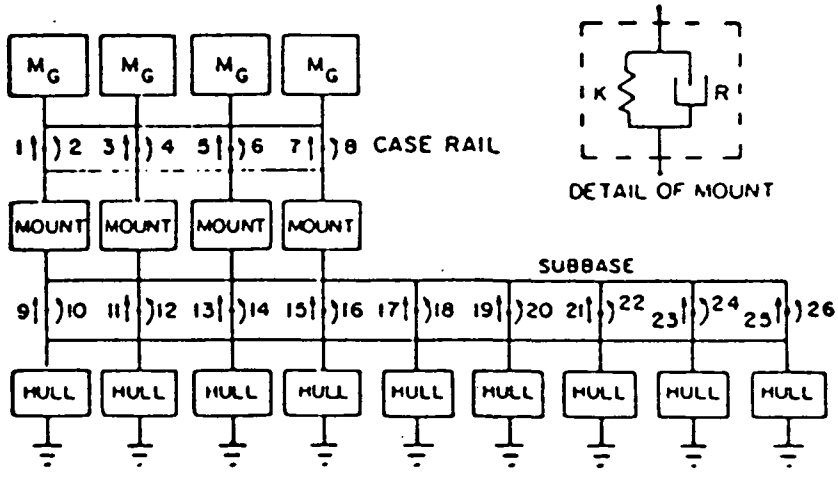

Figure 46. Model of reduction gear mounting system [7]

elements were used to represent the gears, and the case rail was used to model the foundation structure also shown in Figure 45. The two system rested on a set of spring-damper isolator mounts. All these were then supported by a massive beam structure (subbase) which in turn sat on the hull elements modeled as sets of springs and dampers. The cross section of the case rail and subbase are shown in Figure 47. It was also noted that this technique is very similar to the finite element method except here the transfer function used to define the elements are functions of frequency.

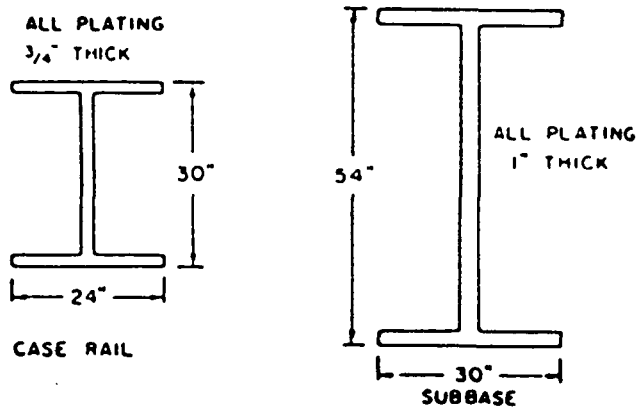

Figure 47. Cross section of the case rail and subbase [7]

The purpose of the above studies on gearbox mounts and suspensions was to obtain parametric design values that will lead to lower force/motion transmissibility. In most gearbox noise and vibration analysis, the mounting system was not taken into account due to the complexity of the gearbox mounts especially in aircraft where the structures are geometrically complex. It is also coupled dynamically to the gearbox and fuselage. However, the inclusion of the mounting system into the dynamic model is a must to obtain a noise and vibration prediction models that truly represent the operating conditions of a gearbox.

F. Overall Gearbox Dynamics [16-18,67]

Noise and vibration prediction and control ideally require an analytical model of the entire gearbox system, its attachments, and other structures connected (i.e. aircraft fuselage, subbase, foundation, etc.in an aircraft application). This is due to the fact that the dynamics of each components which serve as vibrational energy paths may have significant effects on the overall system dynamics. For example, the low to high discrete frequencies excitation generated by the meshing gears in an aircraft are transmitted to the airframe through various structural paths such as the shafts, bearings, housing, mounts, and other attachment points. Discussions in the previous sections of this review have indicated that the dynamics of these structural paths are important to the understanding of the overall dynamics. There is nothing in the literature that offers a rigorous treatment on the overall gearbox dynamics which includes dynamic interactions between the gear-shaft system, support bearings, gear housing, gearbox mounts and suspensions system, and noise radiation. Although, there is a need for such model, many difficulties like allowable model size for computer implementation, complexity of the noise generation mechanism, dynamic coupling between gearbox components, etc. hinder the development of an ideal model. Hence, in most cases one or more components are modeled in detail, and the other parts are modeled with only few degrees of freedom or assumed uncoupled from the rest of the gearbox. These assumptions often limit the applicability of the analysis to specific type of gearbox model such as those discussed in the previous sections.

Berman [67] pointed out the difficulties involved in having a complete dynamical model of the gearbox and fuselage. Some of the problems addressed here are:

1. Cost involved with the assessment of parametric variations
2. Inadequacy of finite element models in the acoustic frequency range

3. High frequency content of the excitations which often excite many modes of the gear-shaft and gear housing system, and so large number of degrees of freedom are needed
4. Complexity of gearbox geometry that is difficult to incorporate, especially in modeling techniques other than finite element methods
5. Difficulty in modeling interface components analytically
6. Problems associated with combining various gearbox component models to form a complete dynamical model

In view of these problems, Berman [67] presented a methodology to be used in the complex gearbox system. It include independent component representation, improvement and development of analytical model using test data, coordinates reduction in the frequency domain, component coupling, and implementation on a computer. In component modeling, each components may be modeled separately using whatever appropriate techniques available, for example finite element model for the gear housing , experimentally obtained impedance matrix to represent the fuselage dynamics, etc. By doing so, each model may be modified without changing the other components.which allows evaluation of design modification to be done easily These models are used with reduced degrees of freedom to synthesize the complete gearbox model in the frequency domain of the form [67]

$$\left([K] - \omega^2[M] - i\omega[C] \right) X(\omega) = F(\omega) \tag{45}$$

where [K], [M], [C], are the stiffness, mass, and damping matrices respectively with $F(\omega)$ as the excitation vector. The reduced component model retains only the interfaces and points of applied force degrees of freedom which usually led to significant reduction in the degrees of freedom. This step of reduction in the degrees of freedom can be shown by

considering a component impedance matrix reordered such that the retained degrees of freedom are in the submatrix z_1 [67]

$$Z(\omega) = \begin{bmatrix} z_1 & z_2 \\ z_2^T & z_4 \end{bmatrix} \tag{46}$$

With some manipulation, the reduced impedance Z_R becomes [67]

$$Z_R(\omega) = z_1 - z_2 z_4^{-1} z_2^T \tag{47}$$

Finally component coupling can be done by the summation of all the relevant degrees of freedom in each components, for example if an interface displacement vector x_i is related to the displacement vector X of the complete system by the expression [67]

$$x_i = T_i X \tag{48}$$

where T_i is the transformation matrix, then the impedance matrix $Z(\omega)$ of the total system would be [67]

$$Z(\omega) = \sum_i T_i^T Z_i T_i \tag{49}$$

A summary of this method is shown in Figure 48. This method was used by Bowes et. al. [17-19], also discussed previously, to model the SH-2D helicopter transmission. The analysis was not entirely analytical, for example the gear housing impedance was derived experimentally due to the problems discussed here and elsewhere. Also there were many

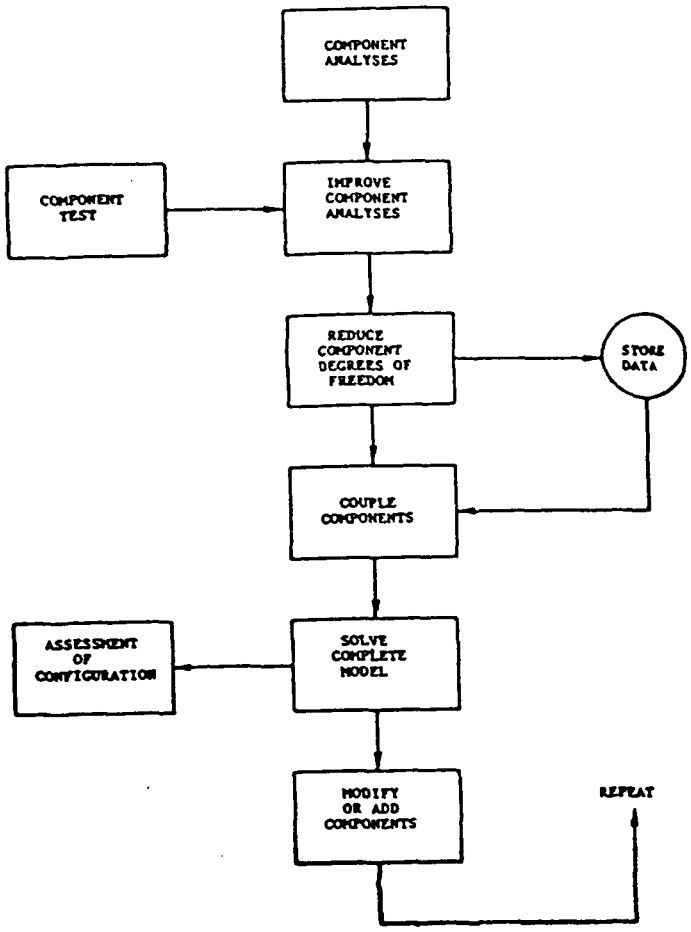

Figure 48. Procedure for dynamic analysis [67]

assumptions like the simple radiation model which did not include environmental effect and housing geometry, and omitted the effects due to gearbox mounts and suspensions. In other gearbox analysis, similar problems also arise. One major difficulty is to be able to model the interface components, such as support bearings, gearbox mounts and suspensions, attachments with simple models yet detail enough to include significant dynamical effects on the entire gearbox system.

G. Design Guidelines [4,5,8,13,14,16-19,29,31,49,52,54,68-74]

Badgley [14] reported that gear mesh excitations are present even in very high quality gears which can be amplified by the resonances in the gear-shaft and gear housing systems. Hence, the vibration and noise sources control alone is not sufficient. In order to effectively control gearbox vibration and noise, design changes in the force/motion transfer paths, i.e. gear body, shaft, support bearing, gear housing, gearbox mount and suspension, and connected structures are inevitable. Also, it is worth mentioning that design modifications in gearbox are very dependable on the gearbox environment, and its application such as helicopter or industrial transmission.

Some design guidelines for noise and vibration control of the gearboxes have been developed in the past. Lack of comprehensive design criteria and proper evaluation techniques have resulted in a number of conflicting requirements as suggested in the literature. This section presents some relevant design criteria for various components of a gearbox other than the gears for reduction in vibration and noise.

G.1. Gear Support System

If the shafts are found to have high amplitude of vibration, stiffening parts of the shafts may reduce the amplitude of vibration especially at the support bearing locations where the force are transmitted to the housing [13,14,17-19,31,68]. This can be done by adding mass around the shafts without increasing the mass center offset, or using materials with high modulus of elasticity - essentially by changing the natural frequencies of the gear-shaft system [29]. It is desirable to have the excitation frequencies away from any natural frequencies as it would be in any design. An example of successful implementation of shaft modification by the addition of mass is shown in Figure 49 where the amplitude of

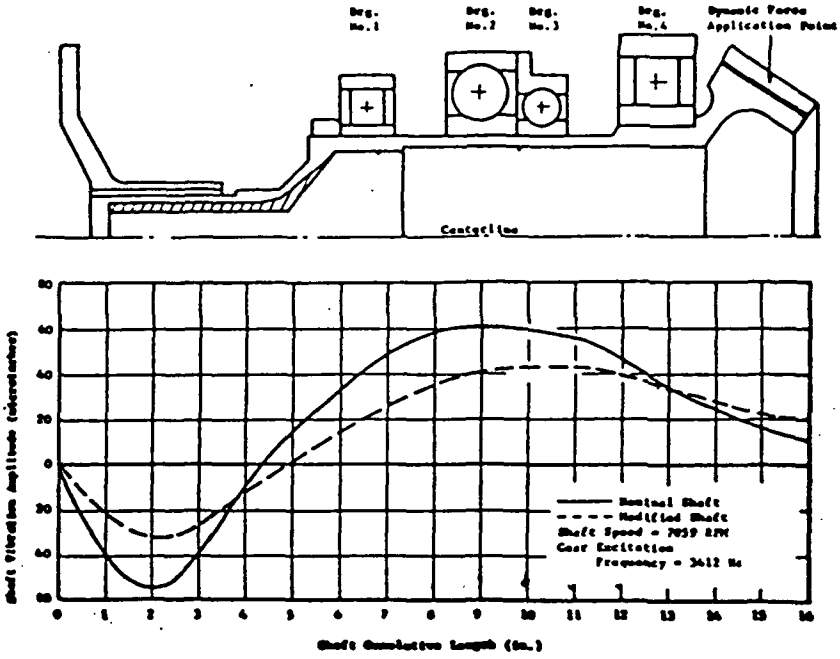

Figure 49. CH-47 transmission shaft vibration amplitudes for nominal and modified configurations [13]

vibration is reduced significantly. Route [69] suggested that when designing a geared transmission system, the highest degree of stiffness permitted by size and weight limitations should be specified.

An alternate method to minimize the force/motion transfer to the housing is to locate the support bearings at the node points on the shafts [4,49,68], and/or support the bearings using stiff frame [29]. By increasing the bearing stiffness with proper choice of bearing type will increase the natural frequencies of the system which may be useful [14,29,31]. Drago [4] noted that gearbox noise level usually decrease with increasing preloads. However, adverse effect may occur in other areas of mechanical design. Figure 50 indicates effect of the shaft support bearings system on the overall noise level. Sleeve bearing are recommended for use as support bearings in gearbox. Although tests have

indicated that the bearing quality in terms of noise reduction is as shown in Figure 50, care must be taken when using such a guideline due to the fact that the performance of these bearings depended on the other gearbox components too. That is, the type of bearing installed will have different effect on the overall gearbox system dynamics by altering the natural frequencies and vibrational energy paths.

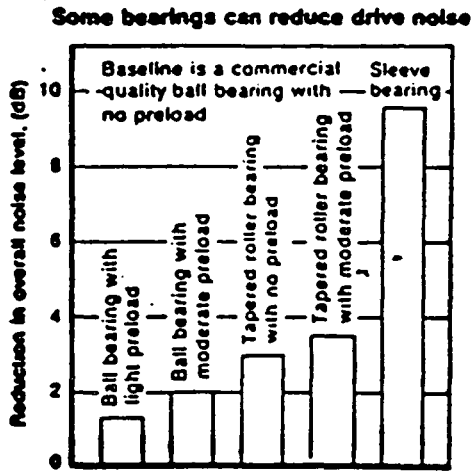

Figure 50. Effect of various bearings on the overall geared transmission noise [4]

Filling of hollow shafts with damping materials is also helpful in reducing the dynamic response of the gear-shaft system when resonance condition exist [14,16,70]. Stemfeld, Schairer and Spencer [16], and Drago [4] tested the effect of damping (elastomeric material) applied to gear body on the overall vibration and noise level. The test results indicated some vibration reduction occurs but not enough to be used alone in design. Hence, it may be used as a supplement to other design changes. Other than the use of damping to absorb vibration, use of vibration absorber has also been suggested to attenuate vibration in the gearbox. The idea of a vibration absorber is that when the absorber is properly tuned, the structure attached stops moving at a particular excitation

frequency. This concept is illustrated in Figure 51 where mode 1 shows the in phase vibration of the absorber and structure at some frequency and mode 2 shows the out of phase vibration with respect to each other at a higher frequency. Hence, somewhere in between at the tuned frequency, the structure will stop moving. Again tests performed on the absorbers indicated that only some reduction in vibration is observed but not significantly to be used alone in design. This is due to the fact that the vibration absorber works only at a particular excitation frequency which is usually varying over a small range. Moreover, there are mesh frequency sidebands which are not attenuated since the absorber is tuned to the mesh frequency only.

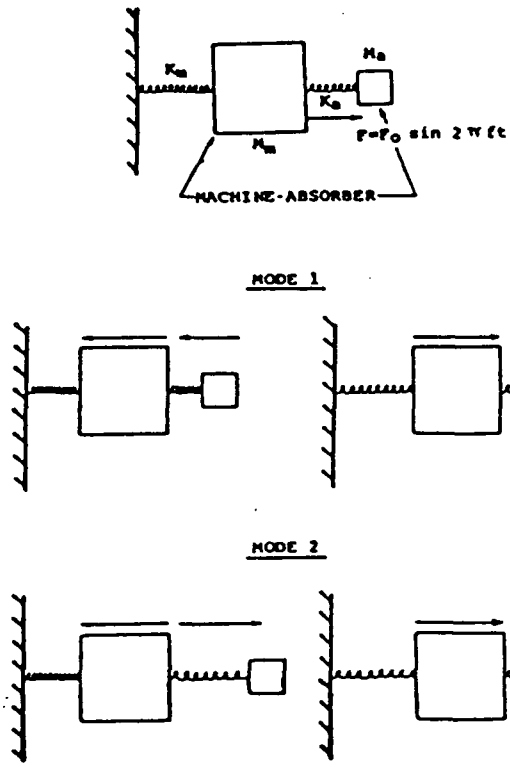

Figure 51. Concept of dynamic vibration absorber [16]

G.2. Gear Housing and Gearbox Mounts

The gear housing is the major noise radiator and also serve as a path for the bearing excitations to the gearbox mounts. Selective stiffening parts of the housing will reduce its vibration amplitude and increase system natural frequencies [4,8,29,68,69,71]. The method used in selecting probable locations for modification in stiffness and mass is discussed in the gear housing dynamics section. The basic idea is to perform a finite element model of the gear housing to identify its natural modes. Then for each mode, the strain energy density is computed and regions with the highest energy density will be selected for this process [4,29] as shown in Figure 33 (section C). This approach allows minimal change in mass and stiffness of the entire gearbox to achieve an amount of increase in natural frequencies.

Over higher frequencies where the radiation efficiency is almost unity, addition of damping through viscoelastic material, and restraint on the gear housing will reduce the mean rms transverse velocity of the housing plate and hence the sound pressure level too [5,29,49,52,72,73]. Effect of various reinforcements added to the a ring gear housing is illustrated in Figure 52. It shows higher reduction in the response for center and ends reinforcement applied together than when applied separately. However, this may not be always possible due to the weight penalty imposed. Addition of mass on the application point of external force, also known as blocking mass method, has shown to reduce noise intensity level of a gearbox as seen from Figure 53.

Some other undesirable gear housing geometries are large flat areas and gently curved surfaces because they usually vibrate freely and are good noise radiator. One way to reduce these effects are to decouple the areas by slotting the housing, add dampers, and thickening the housing [4,5,68]. If weight is not a constraint in the design, the use of cast iron which has good sound absorbing properties is recommended [4]. In terms of structure-borne

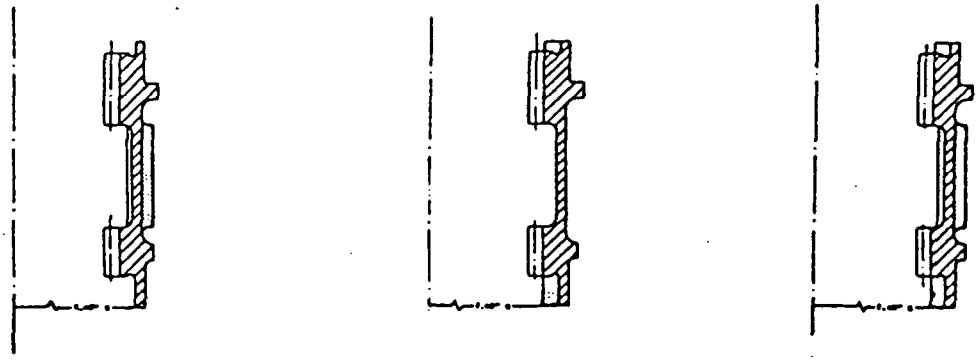

Reinforced Center | Reinforced Ends | Reinforced Center and Ends

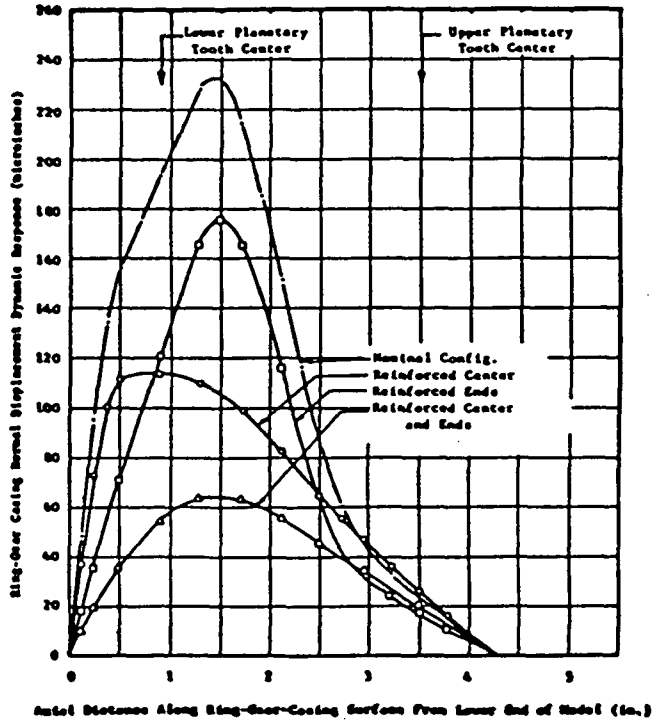

Figure 52. Comparison of ring gear housing vibration amplitude with various reinforcement configurations [13]

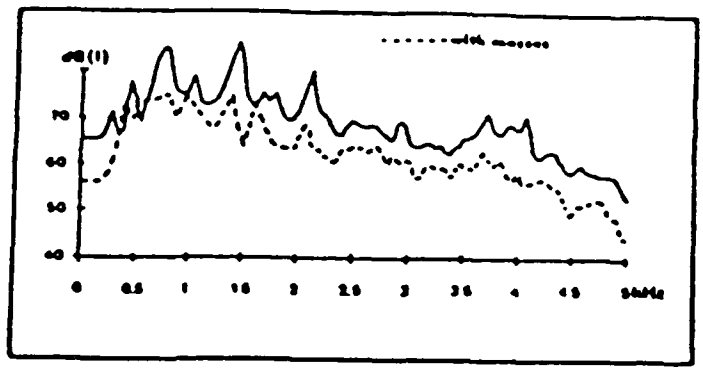

Figure 53. Intensity spectrum of an in-line gear unit, before and after application of blocking mass [52]

paths function, it is better to always supply a rigid load paths between the support bearing locations on the housing and attachments points for the gearbox mounts to reduce housing vibration. Isolators are used to provide resilient support for the gearbox and to reduce force/motion transmissibility through the mounts [54,72,73,74]. This is most useful in marine and industrial type application since a massive foundation can be provided. When designing a mount-isolator system for reduction in force/motion transmissibility, it is desirable to have high mounts and foundation impedances, and low isolator impedance [13].

H. Areas of Further Research

This review indicates that gearbox dynamics and acoustics pose a major problem in the development and implementation of gearbox system technology. The literature confirms this as Mark [1,3], Badgley [11-15,49], Bowes [17-19], Drago [28,29,48,68], Ishida [35], and others have concluded that gearbox noise and vibration levels in aircraft, automobile, etc. are often higher than the allowable limits with respect to human comfort, and machinery failure and life. These problems become more acute at high gearbox operating speed which give rise to excitation frequencies in the order of several kiloHertz as in the aircraft gearbox application. Although many attempts were made to characterize the dynamics of gearbox system components, currently no comprehensive design criteria exist. Moreover, the literature contains conflicting reports concerning relevant design guidelines. All these are mainly due to a lack of the complete understanding of the vibration and noise generating mechanisms of a gearbox system. Hence, further research on gearbox dynamics and acoustics is required.

A major portion of the gear excitation energy is transmitted through structure-borne paths. However, it is difficult to represent the force/motion transfer through the gearbox system analytically and obtain reasonable prediction of the gearbox components vibrational level . It would be useful to be able to characterize the transmissibilities, and to identify the paths quantitatively.

Also, in order to successfully derive the force/motion transfer model, the dynamics of each gearbox components must be known. The bearing subsystem is yet to be modeled with success experimentally or analytically. In addition, the bearing interface models are sometimes difficult to characterize due to its compliance, and the requirement of matching boundary conditions and continuity at the interface. This will lead to better gear-shaft-bearing-housing models.

Another major area which is not well understood is the effect of mounts and suspensions on the force/motion transmissibility and gear-shaft-bearing-housing dynamics. In most gearbox application especially in aircraft, the gearbox are mounted resiliently onto the airframe which is usually light and flexible. Here the vibration is found to be excessive.

The prediction of the noise radiated by the housing and other structures attached will remains a major challenge. This require a model that can relate the structure vibrational level to the sound power radiated. To summarize, the areas related to gearbox dynamics and acoustics which are not well understood are:

1. Bearing dynamics and interface modeling
2. Force/motion transmissibility study including an evaluation of the energy paths
3. Gearbox mount and suspension dynamics and their effects on the overall dynamics and acoustics
4. Noise radiation prediction from housing structure
5. Overall gearbox dynamics and acoustics models
6. Comprehensive gearbox design criteria for reduced noise and vibration

References

1. Mark, W. D., "Gear Noise Origins," AGARD Conference, NATO, Preprint No.369, Lisbon, Port., October 1984.

2. Dale, A. K., "Gear Noise and the Sideband Phenomenon," ASME Paper 84-DET-174, Cambridge, Massachusetts, 1984.

3. Mark, W. D., "Gear Noise Excitation," Engine Noise: Excitation, Vibration, and Radiation, Hickling, R and Kamal, M. M., ed., Plenum Publishing Corporation, New York, pp.55-93, 1982.

4. Drago, R. J., "Gear System Design for Minimum Noise," Gear Noise Seminar, General Motors, February 1986.

5. Dunlap, T. A., and Halvorsen, W. J., "Transmission Noise Reduction," SAE Paper 720735, September 1972.

6. Houser, D. R., "Frequency Spectrum Analysis of Gears," Gear Noise Short Course Notes, The Ohio State University, September, 1987.

7. Lyon, R. H., Machinery Noise and Diagnostics, Butterworth, 1987.

8. Sciarra, J. J., et. al., "Helicopter Transmission Vibration and Noise Reduction Program," Applied Technology Laboratory, USARTL Technical Report 78-2A, Vol.1, Fort Eustis, Virginia, March 1978.

9. Laskin, I., Orcutt, F. K., and Shipley, E. E., "Analysis of Noise Generated by UH-1 Helicopter Transmission," USAAVLABS Technical Report 68-41, Fort Eustis, Virginia, June 1968.

10. Laskin, I. , "Prediction of Gear Noise From Design Data," American Gear Manufacturers Association Semi-Annual Meeting, American Gear Manufacturers Association Paper 299.03, Clayton, Missouri, October, 1968.

11. Badgley, R. H., and Laskin, I., "Program for Helicopter Gearbox Noise Prediction and Reduction," USAAVLABS Technical Report 70-12, Fort Eustis, Virginia, March 1970.

12. Badgley, R. H., "Mechanical Aspects of Gear-Induced Noise in Complete Power Train Systems," ASME Paper 70-WA/DGP-1, 1970.

13. Badgley, R. H., and Chiang, T., "Investigation of Gearbox Design Modifications for Reducing Helicopter Gearbox Noise," Eustis Directorate, USAAMRDL Technical Report 72-6, Fort Eustis, Virginia, March 1972.

14. Badgley, R. H., "Reduction of Noise and Acoustic-Frequency Vibrations in Aircraft Transmissions," 28th. Annual National Forum, American Helicopter Society Preprint No.661, Washington, D. C., May 1972.

15. Badgley, R. H., and Chiang, T., "Reduction of Vibration and Noise Generated by Planetary Ring Gears in Helicopter Aircraft Transmission," ASME Paper 72-PTG-11, 1972.

16. Sternfeld, H., Schairer, J., and Spencer, R., "An Investigation of Helicopter Transmission Noise Reduction by Vibration Absorbers and Damping," Eustis Directorate, USAAMRDL Technical Report 72-34, Fort Eustis, Virginia, August 1972.

17. Bowes, M. A., and Berman, A., "Prediction of Vibration and Noise of a Transmission Using a Dynamic Model Partially Derived from Test Data," Institute of Environmental Sciences, pp.334-338, 1977.

18. Bowes, M. A., "Development and Evaluation of a Method for Predicting the Vibration and Noise Characteristics of Helicopter Transmissions," 33rd. Annual National Forum, American Helicopter Society Preprint No.77.33-76, Washington D. C., May 1977.

19. Bowes, M. A., et. al., "Helicopter Transmission Vibration and Noise Reduction Program," Eustis Directorate, USAAMRDL Technical Report 77-14, Ford Eustis, Virginia, June 1977.

20. Ozguven, H. N., and Houser, D. R., "Mathematical Models Used in Gear Dynamics - A Review," Journal of Sound and Vibration, Vol.121, No.3, March, 1988.

21. Jones, A. B., "A General Theory for Elastically-Constrained Ball and Radial Roller Bearings Under Arbitrary Load and Speed Conditions," Journal of Basic Engineering, ASME, June, 1960.

22. Salzer, M. W., and Smith, J. D., "Real Time Simulation of Gearboxes," Institution of Mechanical Engineers Conference, pp.175-177, 1975.

23. Salzar, M. W., Smith, J. D., and Welbourn, D. B., "Simulation of Noise from Gears when Varying Design and Manufacturing Parameters," World Congress on Gearing, Vol.1, Paris, France, pp.298-308, June 1977.

24. Astridge, D., and Salzer, M., "Gearbox Dynamics - Modeling of a Spiral Bevel Gearbox," Third European Rotorcraft and Power Lift Aircraft Forum, Paper 50, France, pp.1-10, September 1977.

25. Neriya, S. V., Bhat, R. B., and Sankar, T. S., "Effect of Coupled Torsional-Flexural Vibration of a Geared Shaft System on the Dynamic Tooth Load," The Shock and Vibration Bulletin, No.54, Part 3, pp.67-75, June 1984.

26. Hartman, R. M., and Badgley, R. H., "Model 301 HLH/ATC (Heavy Lift Helicopter / Advanced Technology Component) Transmission Noise Reduction Program ," Eustis Directorate, USAAMRDL Technical Report 74-58, Fort Eustis, Virginia, May 1974.

27. Sciarra, J. J. et. al., "Helicopter Transmission Vibration and Noise Reduction Program," Applied Technology Laboratory, USARTL Technical Report 78-2B, Fort Eustis, Virginia, March 1978.

28. Drago, R. J., "New Approach for Analyzing Transmission Noise," Machine Design, Vol.52, No.27, pp.114-115, November 1980.

29. Royal, A. C., Lenski, J. W., Jr., and Drago, R. J., "An Analytical Approach and Selective Stiffening Technique for the Source Reduction of Noise Vibration in Highly

Loaded Mechanical Power-Transmission Systems," 5th. European Rotorcraft and Power Lift Aircraft Forum, Paper 66, Amsterdam, The Netherlands, September 1979.

30. Neriya, S. V., Bhat, R. B., and Sankar, T. S., "Coupled Torsional-Flexural Vibration of a Geared Shaft System Using Finite Element Analysis," The Shock and Vibration Bulletin, No.55, Part 3, pp.13-25, June 1985.

31. Steyer, G. C., "Influence of Gear Train Dynamics on Gear Noise ," Noise-Con 87, The Pennsylvania State University, College Station, Pennsylvania, pp.53-58, June, 1987.

32. Rajab, M. D., "Modeling of the Transmissibility Through Rolling-Element Bearings Under Radial and Moment Loads," Ph.D. Thesis, The Ohio State University, Columbus, Ohio, 1982.

33. Taha, M. M. A., "The Influence of Bearing Misalignment on the Performance of Helicopter Gear Boxes," Wear, Vol.92, No.1, pp.79-97, 1983.

34. Lu, L. K. H., Rockwood, W. B., Warner, P. C., and DeJong, R. G., "An Integrated Gear System Dynamics Analysis Over a Broad Frequency Range," The Shock and Vibration Bulletin, No.55, Part 3, pp.1-11, June 1985.

35. Ishida, K., Matsuda, T., and Fukui, M., "Effect of Gear Box on Noise Reduction of Geared Device," International Symposium on Gearing and Power Transmissions, Tokyo, pp.13-18, 1981.

36. Randall, R. B., "Ceptrum Analysis and Gearbox Fault Diagnosis," Maint. Mng. I., Vol.3, No.3, pp.183, 1982.

37. Randall, R. B., "Separating Excitation and Structural Response Effects in Gearboxes," Third International Conference on Vibrations in Rotating Machinery, Yorkshire,pp.101-107, September 1984.

38. Mitchell, A. M., Oswald, F. B., and Coe, H. H., "Testing of UH-60A Helicopter Transmission in NASA Lewis 2240kW(3000-hp) Facility," NASA Technical Report 2626, 1986.

39. Coy, J. J., et. al., "Identification and Proposed Control of Helicopter Transmission Noise at the Source," Propulsion Directorate, USAAVSCOM Technical Report 87-C-2, March, 1987.

40. Toda, A., and Botman, M., "Planet Indexing in Planetary Gears for Minimum Vibration," ASME Paper 79-DET-73, September 1979.

41. Haustein, B. G., and Schirmer, W., "Utilization of Machinery Housing and Machinery Frame Vibration Sensitivity for noise Reduction," Maschinenbautechnik, Vol.33, No.3, pp.115-119, March 1984.

42. Kato, M., Takatsu, N., and Tobe, T., "Sound Power Measurement of Gear Box by Intensity Method," Second World Congress on Gearing, Vol.1, Paris, France, pp.653-662, March 1986.

43. McFadden, P. D., and Smith, J. D., "Effect of Transmission Path on Measured Gear Vibration," Journal of Vibration, Acoustics, Stress, and Reliability in Design, Vol.108, No.3, pp.377-378, July 1986.

44. Lewicki, D. G., and Coy, J. J., "Vibration Characteristics of OH-58A Helicopter Main Rotor Transmission," NASA Paper 2705, 1987.

45. Singh, R., Houser, D. R., and Zaremsky, G. J., "Modal Analysis of a Gear Housing Plate Using Acoustic Intensity Measurements," Second International Modal Analysis Conference, Orlanda, pp.784-790, February 1984.

46. Van Haven, J., De Wachte, and Vanhonacke, P., "Modal Analysis on Standard Gear Units," ASME Paper 80-C2/DET-79, February, 1980.

47. Croker, D. M., Lalor, N., and Petyt, M., "The Use of Finite Element Techniques for the Prediction of Engine Noise," Institution of Mechanical Engineers Conference, Paper C148/79, Cranfield, pp.131-140, July 1979.

48. Drago, R. J., Lenski, J. W., Jr., and Royal, A. C., "An analytical Approach to the Source Reduction of Noise and Vibration in Highly Loaded Mechanical Power-

Transmission Systems," Fifth World Congress on Theory of Machine and Mechanisms, ASME, pp.910-913, 1979.

49. Badgley, R. H., and Hartman, R.M., "Gearbox Noise Reduction: Prediction and Measurement of Mesh-Frequency Vibrations Within an Operating Helicopter Rotor-Drive Gearbox," Journal of Engineering for Industry, ASME, Vol.96, No.2, pp.567-577, May 1974.

50. Middleton, A. H., "Noise Testing of Gearboxes and Transmissions Using Low Cost Digital Analysis and Control Techniques," SAE Paper 861284, 1986.

51. Beranek, L. L., Noise and Vibration Control, McGraw-Hill, New York, 1971

52. Janssen, L., and De Wachter, L., "Acoustic Intensity Measurements in Aid of the *Design of Gear Casings for Minimal Noise Radiation*," Second World Congress on Gearing, Vol.1, Paris, France, pp.599-604, March 1986.

53. Cremer, L., and Heckl, M, Structure-Borne Noise, Ungar, E. E., ed., Springer-Verlag, Berlin, 1973.

54. Singh, R., "Casing Noise Radiation," Gear Noise Short Course Notes, The Ohio State University, September 1985.

55. Richards, E. J., "Energy Input, Vibrational Level and Machinery Noise; Some Simple Relationships," ASME Paper 81-DET-96, 1982.

56. Seybert, A. F., and Holt, J. A., "A Boundary Element Program for Calculating the Noise Radiated by Vibrating Structures," Noise-Con 85, The Ohio State University, pp.51-56, June 1985.

57. Van de Ponseele, P., Sas, P., and Snoeys, R., "Combination of Structural Modification Techniques and Acoustic Radiation Models," 4th. International Modal Analysis Conference, Union College, Schenectady, New York,Vol.2, Los Angeles, California, pp.943-951, February 1986.

58. Andrews, S. A., "Modern Analysis Techniques Associated with Gearbox and Axle Noise," Institution of Mechanical Engineers Conference, Paper C122/79, pp.47-57, 1979.

59. Umezawa, K., and Houjoh, H., "On the Study of the Sound of Gear and Gear Box Using Acoustical Holography," ASME Paper 80-C2/DET-44, 1980.

60. Hamilton, J. F., "Fundamentals of Vibration and Noise Control by Vibration Isolation," Reduction of Machinery Noise, Crocker, M. J., ed., Purdue University, W. Lafayette, Indiana, pp.81-101, 1973.

61. Snowdon, J. C., Vibration and Shock in Damped Mechanical Systems, John Wiley & Sons, New York, 1968.

62. Warner, P. C., and Wright, D. V., "High Perfomance Vibration Isolation System For the DD 963 Gears," The Shock and Vibration Bulletin, No.45, Part 5, pp.27-42, June 1975.

63. Andrews, R. P., "Gear Case Vibration Isolation in a Geared Turbine Generator," The Shock and Vibration Bulletin, No.54, Part 3, pp.59-65, June 1984.

64. Lunden, R., and Kamph, E., "Vibration Isolation of a Damped Skeletal Machine Foundation - Theory and Experiment," Journal of Acoustical Society of America, Vol.71, No.3, pp.600-607, March, 1982.

65. Granhall, A., and Kihlman, T., "The Use of Mechanical Impedance Data in Predicting Vibration Isolation Efficiency," Noise Control Engineering, pp.88-93, March-April, 1980.

66. Unruh, J. F., "Procedure for Evaluation of Engine Isolators for Reduced Structure-Borne Noise Transmission," Journal of Aircraft, Vol.20, No.1, pp.76-82, 1983.

67. Berman, A., "Transmission of Gear Noise to Aircraft Interiors Prediction Methods," AGARD Conference, NATO, Preprint No.369, Lisbon, Port., October 1984.

68. Drago, R. J., "How to Design Quiet Transmission," Machine Design, pp.175-181, December 1980.

69. Route, W. D., "Seven Design Rules to Help Reduce Gear Noise," SAE Journal, pp.61-67, November 1960.

70. Battezzato, L., and Turra, S., "Possible Technological Answers to New Design Requirements for Power Transmission Systems," AGARD Conference, NATO, Preprint No.369, Lisbon, Port., October 1984.

71. Bensi, G., and Tarricone, L., "Evolution of the Design Techniques for Helicopter Main Transmission Gearboxes," AGARD Conference, NATO, Preprint No.369, Lisbon, Port., October 1984.

72. Grover, E. C., and Anderton, D., "Noise and Vibrations in Transmissions," Engineers Digest, Vol.32, No.9, September 1971.

73. Levine, L. S., "Reducing the Cost Impact of Helicopter Internal Noise Control," 36th. Annual National Forum, American Helicopter Society Preprint No.80-59, Washington, D. C., May 1980.

74. Wang, B. P., and Pilkey, W. D., "On the Optimal Location of Vibration Supports," The Shock and Vibration Bulletin, No.52, Part 5, pp.55-58, May 1982.